THE UNIVERSITY OF OKLAHOMA

GRADUATE COLLEGE

SEPARATE FORMATION ENERGIES OF POSITIVE AND NEGATIVE ION VACANCIES IN LITHIUM FLUORIDE

A DISSERTATION

SUBMITTED TO THE GRADUATE FACULTY

in partial fulfillment of the requirements for the

degree of

DOCTOR OF PHILOSOPHY

BY

OLIVER SANDERS SPENCER

Norman, Oklahoma

1968

SEPARATE FORMATION ENERGIES OF POSITIVE AND NEGATIVE

ION VACANCIES IN LITHIUM FLUORIDE

APPROVED BY

DISSERTATION COMMITTEE

ACKNOWLEDGMENTS

I wish to express my gratitude to Dr. Colin A. Plint, both for suggesting the subject and for the continued interest he has shown throughout this work.

I wish to thank Dr. Stanley E. Babb, Jr., for much assistance in technical matters, and Dr. Chun C. Lin, for helpful counsel.

Last but not least I thank my wife, Rosemary. It is through her faith and patience that I have been able to complete this work.

TABLE OF CONTENTS

LIST OF TABLES

LIST OF FIGURES

SEPARATE FORMATION ENERGIES OF POSITIVE AND NEGATIVE ION VACANCIES IN LITHIUM FLUORIDE

CHAPTER I

INTRODUCTION AND DEFINITIONS

Introduction

In the Born model of an alkali halide crystal it is assumed that the solid is composed of positively and negatively charged ions. The ions adhere to form a stable crystal by virtue of the attractive coulomb forces between the oppositely charged ions, each ion being surrounded by nearest neighbors of opposite sign. The crystal is prevented from collapsing by the short-range repulsive forces which are due chiefly to the Pauli exclusion principle. This model of the alkali halide crystal has enjoyed considerable success in explaining experimental phenomena. Detailed values of the lattice energies and elastic parameters have been calculated for this model.(1)

Nevertheless there is a large body of phenomena which cannot be explained through the assumption that an alkali halide has a perfect ionic lattice; the behavior of the crystal under applied stresses is one example. These phenomena can be explained by assuming that there exist regions in the lattice which depart from the regularity exhibited by an

ideal crystal; that is, there are imperfections in the crystal structure.[2] The understanding of the nature of imperfection leads to a better understanding of the nature of the perfect lattice, and this alone would make their study important. However, some of the most important practical uses of these crystals, such as nuclear particle detectors and cathode-ray tube screens depend upon the nature of imperfections contained within the crystal, which makes the study of imperfections even more important.

In this thesis, consideration will be given to two types of imperfections in alkali halide crystal lattices. The first imperfection is the so-called point defect, a defect which is totally of atomic dimensions and may take several forms. There may be interstitial atoms, impurity atoms, or the absence of an atom normally in the lattice. This last point imperfection is called a vacancy, and will be of special interest in this thesis. In an alkali halide there are two types of vacancies, corresponding to the absence of a positively or a negatively charged ion from its proper place in the lattice. These are called cation and anion vacancies respectively.

The second type of defect is a one-dimensional imperfection, and is known as a dislocation. The dislocation is a line defect and has one dimension that is macroscopic. It is thermodynamically unstable and may be removed by annealing the crystal. On the other hand, a vacancy may be present in thermodynamic equilibrium; in fact, at temperatures above absolute zero, vacancies must be present so that there can be thermodynamic equilibrium.

There are electrical effects associated with each type of defect; these electrical effects will be introduced and discussed later in the thesis. The measurement of these effects allows the calculation of some basic quantities relating to defects in alkali halide crystals, and to lithium fluoride in particular.

Point Defects[3]

Schottky Defects

Consider an ionic crystal at some temperature T above absolute zero. We assume that the crystal has the rocksalt structure, although this is not necessary for the following calculation. There will be an equal number of cation and anion sites, denoted by N. We now introduce a number of vacancies into the crystal as follows: A cation and an anion are removed from their positions in the interior of the crystal and placed far apart on its exterior surface, or in the core of a dislocation inside the crystal. It is generally accepted that a dislocation can act as a source or sink for vacancies in this manner. In order that the interior of the crystal remain electrically neutral, we must have as many anion vacancies as cation vacancies. Thus we must create anion and cation vacancy pairs rather than individual vacancies.

If n cation and anion vacancies are created simultaneously we want to know the value of n that will exist when the crystal is in thermodynamic equilibrium at T. The equilibrium value of n is determined by minimizing the part of the Gibb's free energy due to the introduction of the vacancies. If E is the energy of formation of a

vacancy pair and S is the configurational entropy charge which accompanies the formation of the n vacancy pairs in the crystal, then Gibb's free energy due to the n vacancy pairs can be written as

$$\Delta g = nE - ST \quad . \tag{1}$$

We neglect any terms associated with volume changes since these are small relative to the energy and entropy terms.

The configurational entropy term can be written as

$$S = k \ln\left(\frac{N!}{(N-n)!n!} - \frac{N!}{(N-n)!n!} \right) \tag{2}$$

where the first factor is the number of ways of arranging the n cation vacancies on the N cation sites in the crystal, and the second factor is the number of ways of arranging the anion vacancies on the anion sublattice. When Equation (2) is put into Equation (1) and the resulting expression minimized with respect to n in the standard manner, the following expression for the equilibrium number of vacancies at temperature T results:

$$\left(\frac{n}{N} \right)\left(\frac{n}{N} \right) = \exp\left(- \frac{E}{kT} \right) \tag{3}$$

Thus at any temperature above absolute zero, there will be a number of vacancies present in the lattice; these vacancies must be present so that the crystal will be in thermodynamic equilibrium. It

should be noted that the energy of formation E is the sum of the individual energies of formation of anion and cation vacancies. Nothing concerning the individual energies of formation can be determined from this expression. The reason for leaving Equation (3) in the above form is to stress the fact that it is analogous to a solubility product relation. This form shows that the product of the fraction of anion vacancies and the fraction of cation vacancies is equal to

$$\exp(-\frac{E}{kT})$$

even when the two fractions are unequal, as may be the case when there are vacancies due to other causes in the crystal.

Frenkel Defects

The Frenkel defect occurs when an ion leaves its proper lattice position and goes into an interstitial position. Two defect types are thus created: interstitial ions and their accompanying vacancies. The calculated formation energy for Frenkel defects is much larger than that for Schottky defects in the alkali halides. Even after divalent atoms are added to the crystal, there is a negligible number of Frenkel defects in the lattice. For this reason, a detailed consideration of Frenkel defects will not be carried out, although the calculation of their equilibrium number in the lattice at temperature goes exactly as Equation (3), and yields a similar result.

Divalent Impurities

The atoms which make up the pure alkali halide crystal are univalent; that is, the absolute value of the charge on an ion is equal to one electronic charge in magnitude. When a divalent impurity atom is introduced into a otherwise perfect alkali halide crystal, there is evidence to indicate that it enters the lattice substitutionally, displacing one of the atoms which carries the same sign as itself. In order that charge neutrality be preserved in the crystal, a vacancy is also formed. Thus the introduction of a divalent impurity atom into the alkali halide lattice leads to the formation of a vacancy having the opposite sign to that of the impurity atom. It follows then, that if a concentration c of divalent impurity atoms is introduced into the crystal, there will also be an equal concentration c of vacancies accompanying them. Two kinds of point defects are put into the crystal; the impurity atom and its accompanying vacancy. These may be associated with each other or may act independently.

At a sufficiently high temperature a vacancy can become separated from the accompanying impurity atom and diffuse through the crystal as if it were an independent entity. Below this temperature, a certain number of the vacancies and the impurity atoms are associated with each other. Since the impurity atoms are relatively immobile at all temperatures, this association renders the vacancy immobile. There is then at a given temperature a maximum of c vacancies per unit volume due to the presence of a concentration c of divalent impurities.

Ionic Conductivity

The presence of vacancies in an alkali halide crystal can be connected directly to the ionic conductivity of the crystal.[4] It is found that the graph of ionic conductivity versus inverse temperature divide into two easily distinguishable regions above, say, 300°C. These regions have been found to correspond to conduction dominated by vacancies generated by different mechanisms. In the lower temperature region, the majority of the vacancies are those which accompany the divalent impurities in the crystal. At the higher temperatures the vacancies are thermally generated. We will not be concerned with that temperature region below about 300°C, where association of impurities with vacancies occurs, except incidentally. Even though impurity-vacancy association has been extensively investigated, the temperatures of interest to this thesis are those which lie between 300°C and the melting point of the crystal.

The two different regions of the ionic conductivity can be most clearly seen when the natural logarithm of the product of ionic conductivity and temperature is plotted versus the inverse of the temperature. Such a graph will be called a conductivity plot. In this plot the two extreme regions appear as straight lines with different slopes with a transition region between them. The lower temperature part of the plot is known as the extrinsic, or structure sensitive retion; the higher temperature part is known as the intrinsic region.

Since the extrinsic conductivity region is controlled by the presence of impurities, it varies from crystal to crystal; however, the ionic conductivity in the intrinsic region is controlled only by the Schottky defects and consequently does not vary from sample to sample of the same material. It is possible to dope a crystal so heavily with divalent impurities that it will not enter the intrinsic region at any temperature below the melting point.

The temperature at which the number of thermally generated vacancies equals the number of impurity generated vacancies is known as the transition or knee temperature T_k. Below this temperature the ionic conductivity is of the extrinsic type; above this temperature, it is intrinsic. T_k is found by extending the straight lines of the conductivity plot until they intersect; the temperature of the intersection point is T_k. Since at this temperature n = c, we may write

$$c = \exp\left(-\frac{E}{2kT_k}\right) \tag{4}$$

which gives the number of divalent impurities in the crystal as a function of T_k.

Dislocations

General Properties

When a crystal is subjected to tension or compression, there will first be a region where the stress and strain are linearly related. If the stress is removed, the crystal will return to its original shape, none the worse for wear. However, if more stress is applied to the crystal, a region of stress will be reached where the stress and strain are not related linearly, and the strain in the crystal will be irreversible. This is the region of plastic flow in the crystal. The stress-strain plot of a particular specimen depends on a number of factors such as the temperature, the history of the specimen, and the impurity content. Sharp transitions from elastic to the plastic regions usually do not occur, but it is possible to define a certain critical shear stress where plastic flow will set in. However, it is more satisfactory to define a quantity known as the critical resolved shear stress.[5] This quantity is the stress above which plasticity begins in the form of slip on a given slip system; that is, when the crystal begins to slip along a particular direction in a certain plane. The slip system is specified by giving both the slip plane and the slip direction. The Schmid law of the critical resolved shear stress[2] states that slip takes place along a given slip system when the shear stress on that system reaches a critical value; in many solids, this slip system consists of the planes having the widest spacing, but in the alkali halides, the slip plane is the

(110) plane, and the slip direction is $[\bar{1}10]$. All of the planes and directions which can be transformed into this slip system by the symmetry operations of the crystal are also candidates for slip systems.

In the theoretical approach to the explanation of plastic deformation it was originally assumed that planes of atoms slipped over one another as rigid planes.[2] Slip was considered to occur simultaneously over all parts of the plane. The value obtained for the shear stress using this assumption was, however, as much as five orders of magnitude greater than experimentally determined values. Since slip always accompanies plastic deformation, this discrepancy has lead to the hypothesis that slip does not occur simultaneously over the entire slip plane, but begins at a particular place and propagates through the crystal on the slip planes. The concept of the dislocation as the mechanism which transmits slip through the crystal was introduced in 1934;[6] since then the dislocation has been widely used to explain plastic flow and other properties of solids.

The dislocation is a line imperfection; in the alkali halides it has two extreme forms, the edge dislocation and the screw dislocation. A dislocation may also be intermediate between these two extremes; it may have some edge and some screw character. Excellent presentations of dislocation theory have been given by Read[7] and Cottrell,[8] so we will only give a summary of their properties here.

The edge dislocation is shown in Figure 1. Above the slip plane there are n vertical atomic planes; below, there are n - 1

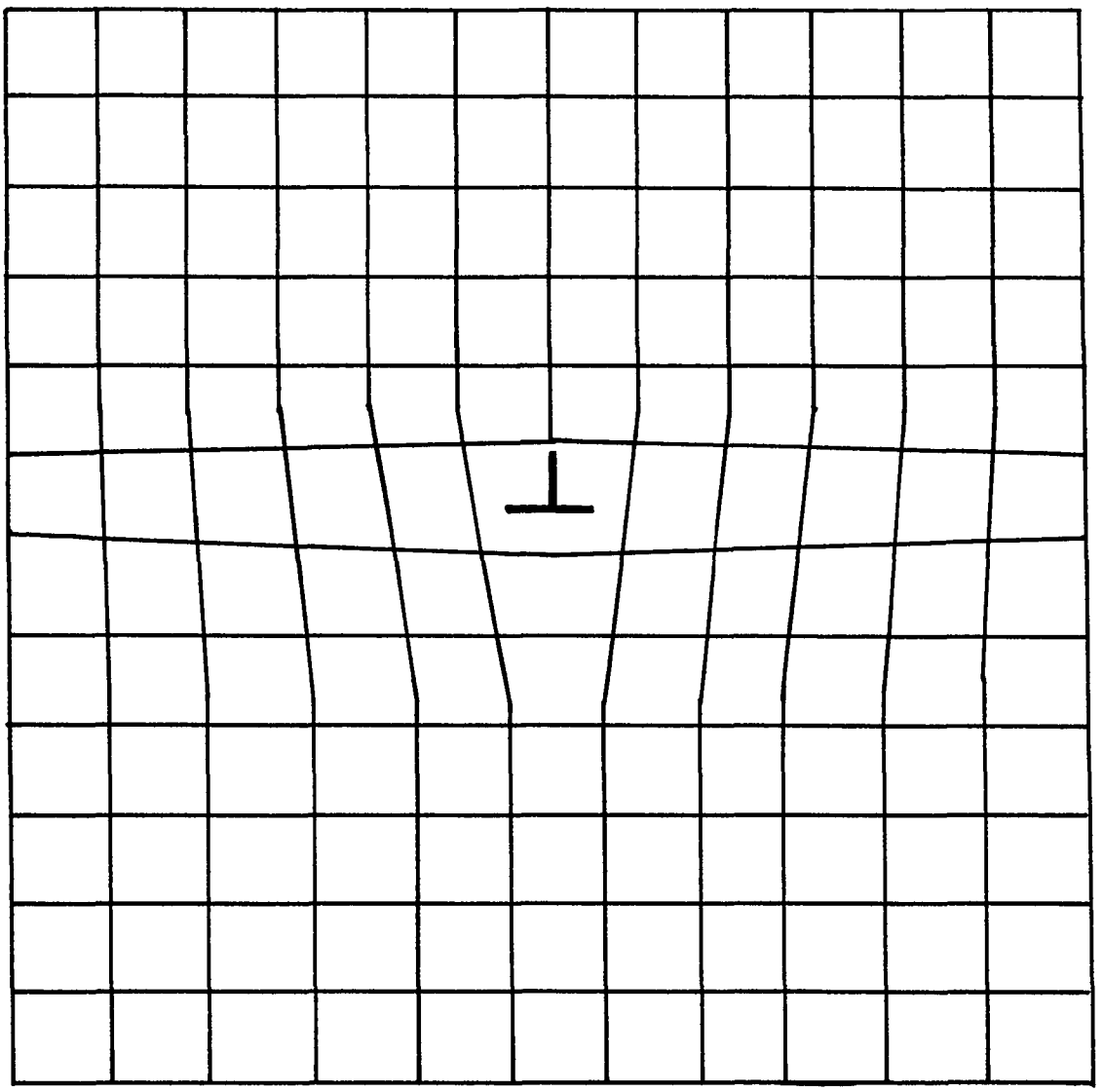

FIGURE 1. AN EDGE DISLOCATION

planes. The edge dislocation, denoted by $\perp$, is the terminating edge of an extra half-plane of atoms in the crystal. The region of the edge is called the core of the dislocation, and the termination plane is called the slip plane. It is the plane on which the dislocation can move freely. The Burgers vector of a dislocation has a magnitude which gives the amount by which the material above the slip plane is displaced with respect to that below; its direction is the direction of this displacement. The Burgers vector of an edge dislocation is perpendicular to the core of the dislocation.

The simplest way of determining the Burgers vector of a given dislocation is by using the so-called Burgers circuit, which is formed as follows. A circuit is traversed in regions far from any dislocations by connecting lattice points of the real crystal. The circuit must be such that it would be closed if the crystal were perfect. Consider, however, the case that one dislocation is contained within the circuit; then, the circuit would not close, and the vector drawn from the starting point to the finish of the unclosed circuit will be the Burgers vector of the dislocation. The direction of the Burgers vector thus depends on the direction in which we decide to traverse the circuit, which corresponds to the uncertainty in our knowledge of which side of the slip plane is to be considered unslipped. The Burgers vector of an edge dislocation is perpendicular to the extra half-plane of atoms. The magnitude of the Burgers vector is known as the strength of the dislocation.

To visualize a screw dislocation, consider an imaginary set of discs stacked in the crystal, as in Figure 2a. Then cut the discs along the direction specified by the Burgers vector as in Figure 2b. It can be seen that this operation transforms the originally plane surfaces of the discs into a single helicoidal surface; thus, no plane can be singled out as the extra half plane. For a screw dislocation, the Burgers vector is parallel to the core of the dislocation.

Even though there are other types of dislocations, in particular the so-called partial dislocations, these will not occur in the alkali halides because of the requirement that adjacent atoms have opposite charge; thus we will ignore them here.

Dislocations in Alkali Halides

The physical properties of alkali halides are not as affected by the presence of dislocations as in the case of metals, but the effects have the enormous advantage that they can be studied directly. The electron cloud that gives metals their most interesting properties also renders direct observation of interior dislocations impossible. On the other hand, the alkali halides are quite transparent over a wide spectral range, allowing one to study, among other things, the effect of dislocations on the optical properties of the crystals.

Gilman and Johnston[9] have studied the properties of the dislocations in lithium fluoride and have determined the influence of dislocations upon many of the physical properties of this material. In

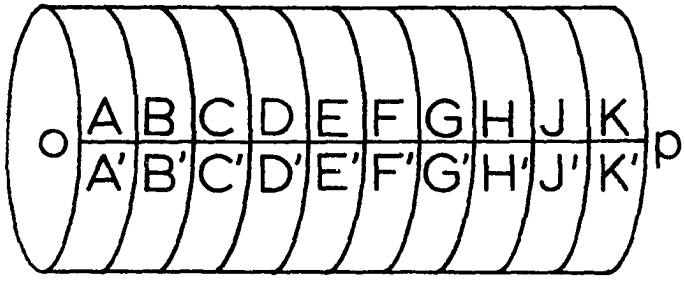

a. Discs cut from atomic planes in a dislocation-free crystal.

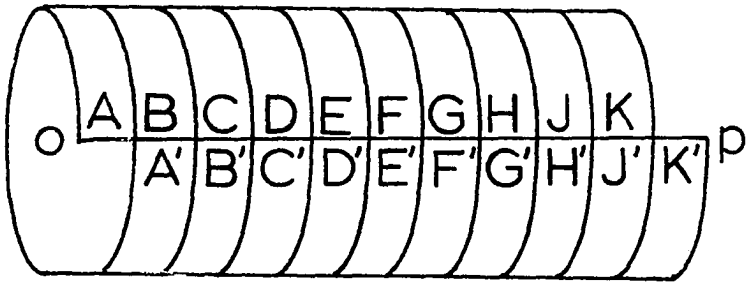

b. The modification that occurs when a screw dislocation passes through the discs.

Figure 2. A screw dislocation

particular, they found that the plastic deformation of the crystal was accompanied by dislocation motion. The creation of new dislocations took place by the so-called "multiple cross-glide" mechanism, and the freshly created dislocations were the ones responsible for the plastic properties of the crystal. The older dislocations were shown to be ineffective in plastic deformation; they were apparently pinned by impurity atoms. Gilman and Johnston did not study the mechanism of dislocation pinning in lithium fluoride closely, but did note that there seemed to be a migration of impurities into the region of the dislocation.

Dislocations in alkali halides are somewhat different from dislocations in metals. Due to the stringent requirement of charge conservation in these crystals, it is more correct to consider two half planes of opposite charge as comprising a dislocation than to consider only a single half plane as in metals.[10] This feature of the dislocations in alkali halides leads to the possibility of charged dislocations. An edge dislocation in an alkali halide having the rocksalt structure is shown in Figure 3.

As in metals, the screw dislocation has no unique slip plane associated with it. Whereas the edge dislocation has a half plane that is constrained usually to move parallel to a given set of planes, the screw dislocation is not constrained in this manner. One feature of the screw dislocation is that it carries no charge in the dislocation core. In addition, Gilman and Johnston[9] found the velocity of screw dislocations in lithium fluoride to be some fifty times smaller than the velocity of edge dislocations.

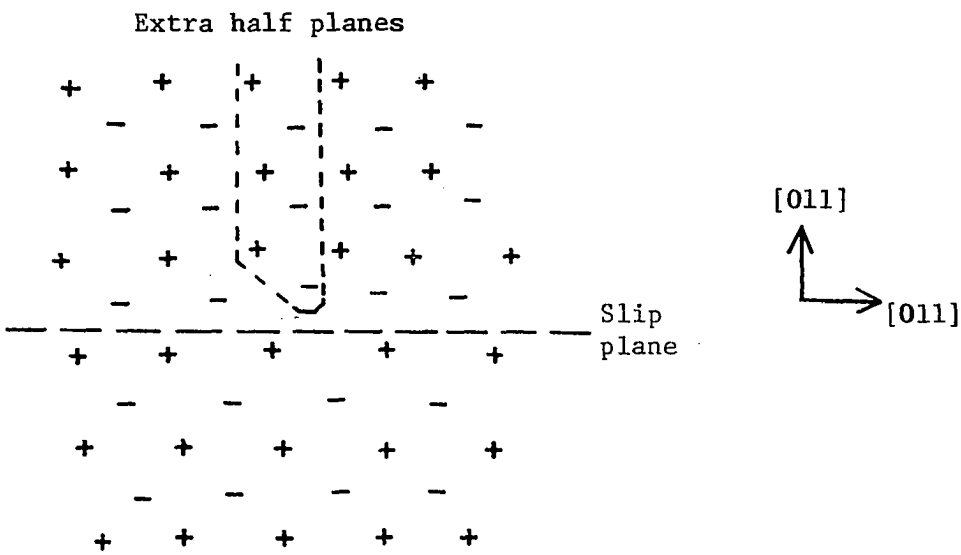

Figure 3. Edge dislocation in rocksalt structure.

Dislocations and Bending

Dislocation Motion in Plastic Deformation

Dislocations were originally introduced to explain the low yield stress of crystals. The passage of a dislocation through a crystal will cause slip to occur, making the yield stress much lower than if entire planes of atoms slid unchanged over each other. Dislocations are now the basis for understanding many mechanical properties of solids. A crystal's resistance to dislocation motion determines largely its hardness and ductility; grain boundary formation is explained on the basis of dislocations stacked one above the other. That the dislocation concept is probably correct is indicated by the observation that any treatment that alters the ability of the dislocation to move also affects the yield strength of the crystal. Dislocation motion accompanies all types of plastic flow. A normally soft material can become brittle if so many dislocations are introduced into it that they impede one another's motion. Copper, for example, is a soft material; introducing dislocations by cold working causes it to become brittle and break rather than to continue to yield to increasing stress.

Tension and Compression

The slip system in the alkali halides having the rocksalt structure is along the [101] direction in the $(10\bar{1})$ type planes. It must be recognized that there are some 6 equivalent (110) type planes,

any of which may be a slip plane; that particular (110) plane on which the resolved shear stress first reaches the critical value will be the slip plane for any applied stress. If we apply a tensile or compressive stress normal to the (001) planes, using the geometry of Figure 4, there will be four operative slip systems. Take the compression case as an example. The operative slip systems will then be $[0\bar{1}1](011)$, $[011](0\bar{1}1)$, $[101](\bar{1}01)$, and $[101](101)$. The numbers in brackets indicate the direction of slip; the numbers in parentheses indicate the planes along which slip occurs. In this case the critical resolved shear stress will be reached simultaneously on four slip systems due to the symmetry of the situation. Dislocation motion on any of the four slip systems is equally likely in the case of plastic deformation. We may then say that a sufficiently large stress in the [001] type direction will result in dislocation motion along the (100) type planes in crystals having the rocksalt structure.

It should be noted that a given amount of slip may be arrived at in two different ways. For example, if a dislocation of Burgers vector b moves through the crystal in the direction as shown in Figure 5a, the same result can be achieved by motion of a dislocation of Burgers vector -b in the opposite direction. Even though the slip plane is the same in both cases, and the amount of slip also the same, the final situation is reached by having dislocations moving in opposite directions. We say that these dislocations have opposite mechanical signs. Thus, for a given slip plane, dislocations having opposite mechanical signs will move in opposite directions in response to the same applied stress.

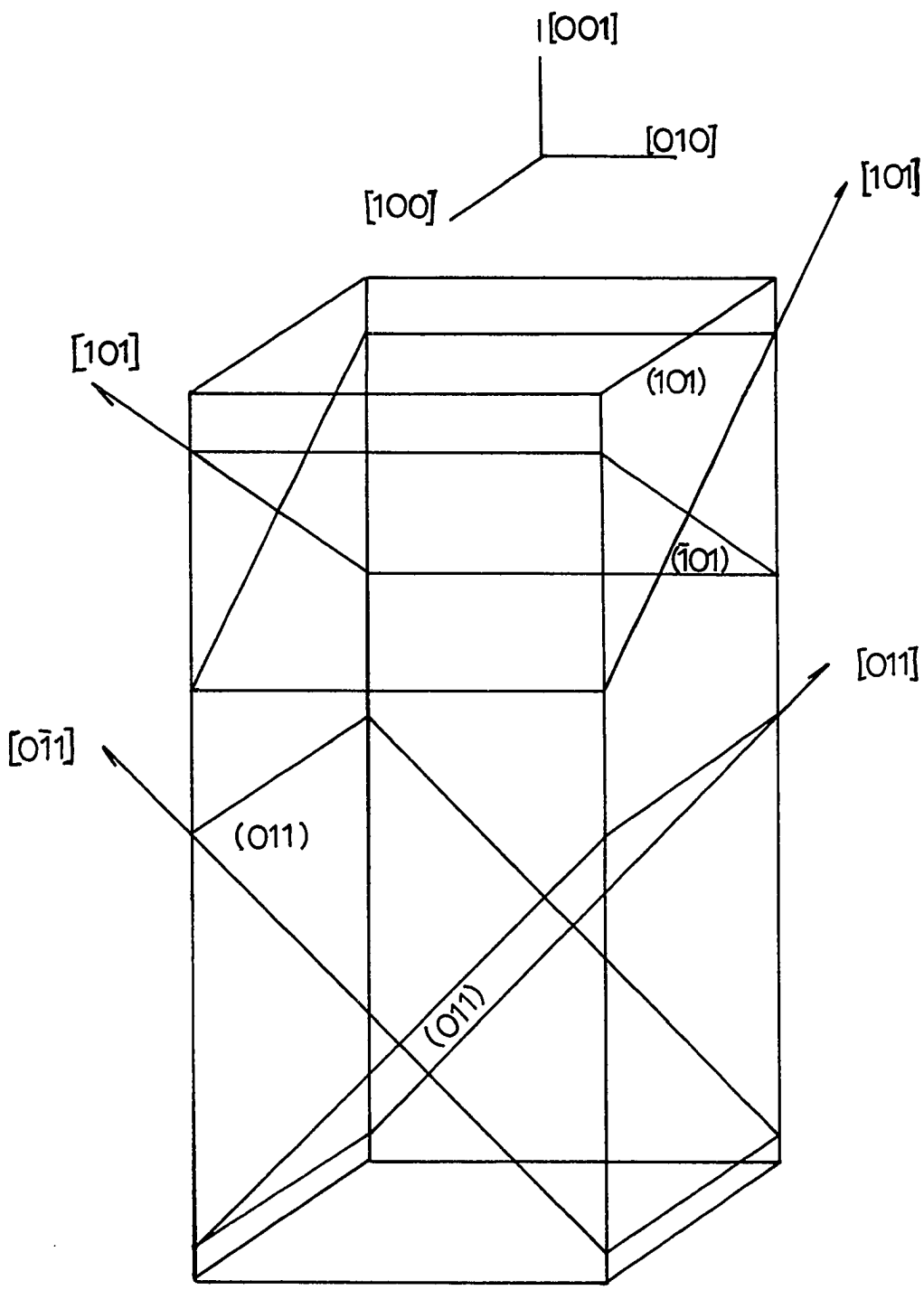

FIGURE 4. SLIP PLANES IN COMPRESSION FOR THE ROCKSALT STRUCTURE

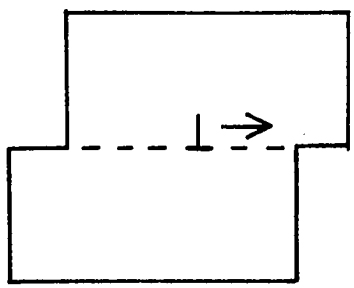

a. Slip produced by a positive edge dislocation moving to the right.

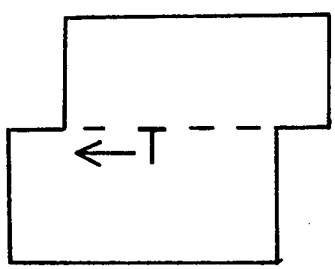

b. Slip produced by a negative edge dislocation moving to the left.

Figure 5. Dislocations of different mechanical sign

In the compressive stress situation discussed above, the same strain would have been created by dislocations moving in opposite directions from those mentioned, but having their extra half plane on the other side of the slip plane.

Bending

In the case of bending[11] the situation becomes more complex. Consider the geometry of Figure 6. The bending axis is in the [010] direction, and the long axis of the crystal is in the [001] direction. The tension face is then the (100) face, while the compression face is the $(\bar{1}00)$ face. As in all cases of pure bending, there is a plane roughly halfway between the tension and compression faces which has no stress. This plane is known as the neutral plane. The stress varies from a maximum tensile stress on the (100) face, to zero stress on the neutral plane, to maximum compressive stress on the $(\bar{1}00)$ face.

Using the geometry so outlined, two dimensional bending is defined as that mode of bending which results in the motion of dislocations along the (101) and $(10\bar{1})$ planes. The bending is termed two dimensional since the bending takes place in one plane. The strain in the crystal is such that the crystal is bent about an axis parallel to the bending axis of the applied stress.

Since the dislocations are nucleated in the regions of highest applied stress, they will be formed near the tension and compressionion faces of the crystal. The dislocations having one mechanical sign will move in one direction, and those of the opposite mechanical

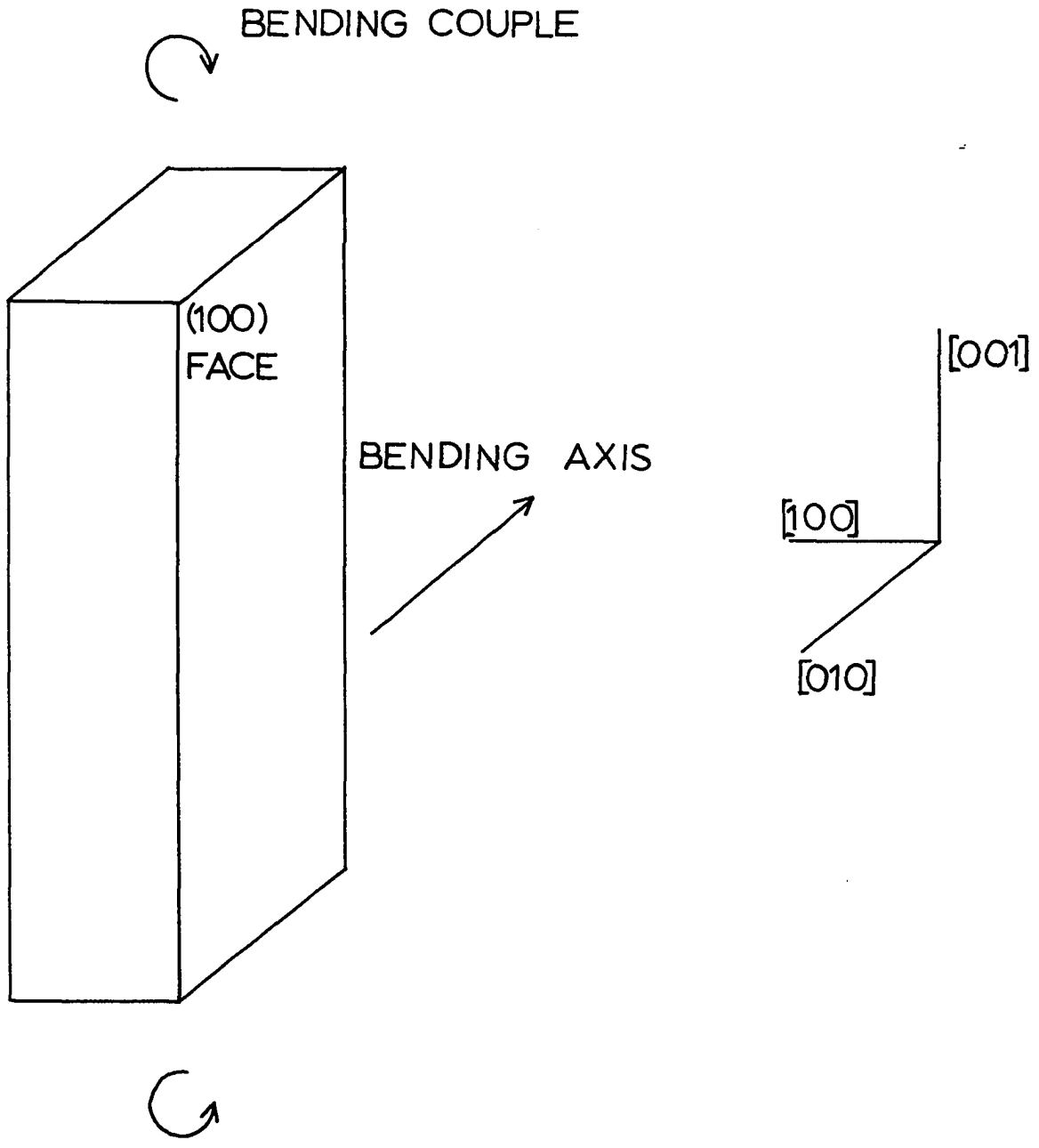

FIGURE 6. BENDING GEOMETRY

sign will move in the opposite direction. The dislocations moving toward the neutral axis will proceed inward until they reach a point where the stress is not large enough to sustain further motion. Dislocations of the opposite mechanical sign will move out of the crystal.

The dislocation motion to be expected in the two dimensional mode of bending is shown in Figure 7, where $\perp$ denotes an edge type dislocation (with the perpendicular bar showing the extension of the extra half plane), and $\circlearrowright$ denotes a screw dislocation. It may be seen in this figure that the dislocations approaching the neutral axis from opposite sides have the same mechanical sign. Thus, if pure bending of the crystal takes place in the two dimensional mode, the resulting dislocation density will have an excess of dislocations of the same mechanical sign located in the neighborhood of the neutral axis.

There is another mode of bending that can occur in the same geometry. Three dimensional bending is defined to be bending that involves dislocation motion on the (011) and $(0\bar{1}1)$ planes. In this bending mode, the crystal strain causes the crystal to be bent about an axis that has a component perpendicular to the bending axis of the applied stress. The dislocation motion that accompanies three dimensional bending is shown in Figure 8. Hikata et al.[12] have shown that if the dimension of the crystal is small in the [100] direction, then the amount of bending in the three dimensional mode will be small; this will be the case in the work discussed in this thesis.

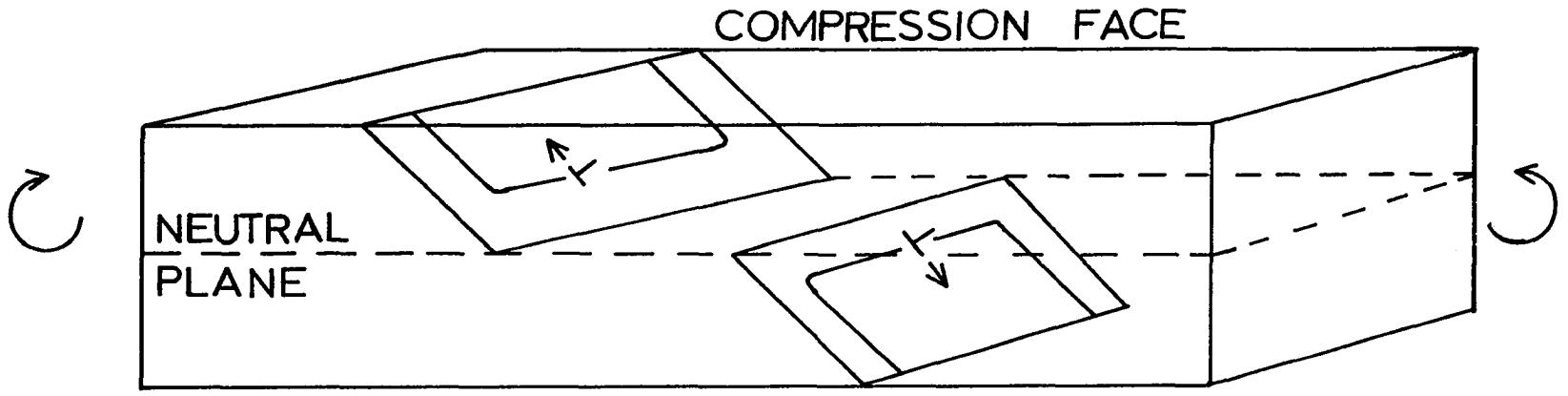

FIGURE 7. DISLOCATION MOTION IN TWO-DIMENSIONAL BENDING.

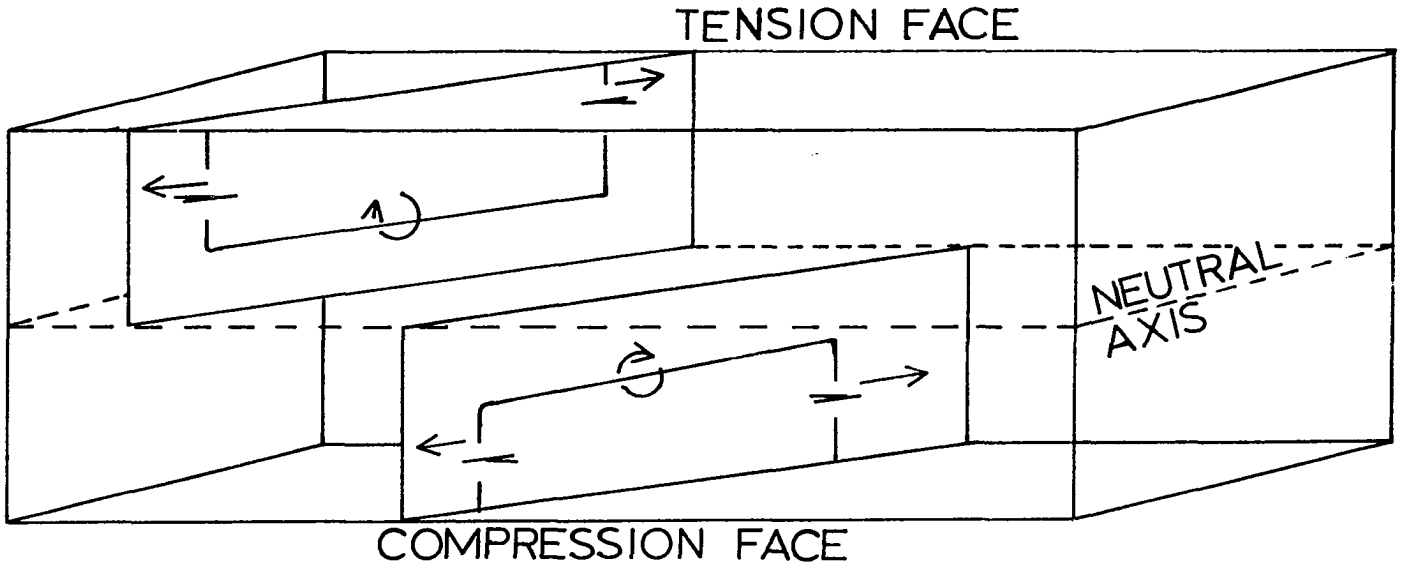

FIGURE 8. DISLOCATION MOTION IN THREE-DIMENSIONAL BENDING

CHAPTER II

THEORY OF IONIC CONDUCTIVITY

General Considerations

Pure ionic conductivity results in the liberation of the components of the ionic material at the rate of one gram equivalent weight for each Faraday of charge passed through it. Tubandt[13] used this fact to demonstrate that the alkali halides are ionic conductors. He also determined the transport numbers of several alkali halides. The transport number of a component is the fraction of the current carried by that component. To an excellent approximation for the alkali halides, the transport numbers are unity for cations and zero for anions.

A number of experiments have been carried out to determine the temperature dependence of the ionic conductivity of the alkali halides. In all of the experiments, the conductivity plot is best fitted by a superposition of two straight lines. In what follows we will restrict ourselves to temperatures above 300°C, since at lower temperatures the vacancies and divalent impurities form complexes.

At the lower end of the conductivity plot, the conductivity varies with temperature as

$$\sigma(\text{low temperature}) = A_1 \exp(-E_1/kT) \tag{5}$$

while at the upper end of the curve, the conductivity varies with temperature as

$$\sigma(\text{high temperature}) = A_2 \exp(-E_2/kT) \tag{6}$$

where E_1 is less than E_2, and A_1 is much less than A_2. It is an experimental fact that the value of A_1 is sensitive to the amount of divalent impurity in the specimen, while A_2 is not affected. From its form, then, the ionic conductivity appears to be a thermally activated process with two active elements. The lower temperature region of the conductivity plot is called the extrinsic region, while the high temperature region is called the intrinsic.

Vacancies

As mentioned earlier, the ionic conductivity of an alkali halide is strongly dependent on the number of positive ion vacancies present at a given temperature. The participation of a given cation in the conductivity is governed by its ability to move into a proper lattice site; the probability of this site being unoccupied depends on the number of vacancies in the lattice, whether of thermal or impurity origin. Thus an increase in the number of vacancies increases the number of cations able to move in any given period of time, and thereby increases the conductivity.

Mobility

The expression for the conductivity is, in general,

$$\sigma = xq\mu \tag{7}$$

where x is the number of charge carriers per unit volume, q is the charge and μ is the mobility of the carriers. It has been shown[14] by statistical thermodynamics that the mobility of a cation as a function of temperature is

$$\mu = \frac{B}{T} \exp(-U/kT) \ . \tag{8}$$

It is seen that the mobility is also a thermally activated process.

General Expression for the Ionic Conductivity

Equation (7) of chapter I gives the number of positive and negative ion vacancy pairs at temperature T. This equation was left in the solubility product form to emphasize that it is obeyed regardless of the number of vacancies already in the crystal. For convenience, this expression can be rewritten in the form

$$x_1 x_2 = x_0^2 \equiv \exp(-E/kt) \ , \tag{9}$$

where x_1 is the concentration of positive ion vacancies and x_2 is the negative ion vacancy concentration. As before, E is the formation energy of an isolated ion pair.

For a pure crystal, $x_1 = x_2$. This reflects the electro-neutrality condition of the alkali halides. In the presence of a concentration c of positive ion vacancies caused by impurities, the condition of charge neutrality is

$$x_1 = x_2 + c \ . \tag{10}$$

Upon combining this with expression (9) we get

$$x_1(x_1 - c) = x_0^2 \ , \tag{11}$$

Solving for x_1, we get

$$x_1 = \frac{c}{2} \left[1 + \left(1 + \frac{4x_0^2}{c^2}\right)^{\frac{1}{2}}\right] \ . \tag{12}$$

Thus the expression for the conductivity is, using (7), (8) and (12):

$$\sigma = \frac{qB}{2T} \left\{c + \left[c^2 + 4\exp(-E/kT)\right]^{\frac{1}{2}}\right\} \exp\left(-\frac{U}{kT}\right) \tag{13}$$

At low temperatures $4\exp\left(-\frac{E}{kT}\right) << c^2$, so

$$\sigma(\text{low temperature}) = q \frac{Bc}{T} \exp(-U/kt) \ , \tag{14}$$

while at high temperatures $4\exp\left(-\frac{E}{kT}\right) << c^2$, so

$$\sigma(\text{high temperature}) = q \frac{B}{T} \exp\left(-\frac{U+E/2}{kT}\right) \tag{15}$$

From Equation (14) we see that a plot of $\ln\sigma T$ vs. $1/kT$ will have a slope of $-U$; the same plot for Equation (15) will have a slope of $-(2U+E)/2$. Thus Equation (13) does show the two conductivity regions demanded by experiment.

Determination of Quantities in the Expression for σ

U is easily determined by measuring the slope of the ln T vs. $1/kT$ plot in the low temperature region. Now E is the sum of the individual energies of formation of positive and negative ion vacancies;

$$E = g_+ + g_- \tag{16}$$

and as is usual, it is assumed that the free energies of formation can be written in the following manner:

$$g_+ = g_+^\circ - kT\ell nA_+ \tag{17}$$

$$g_- = g_-^\circ - kT\ell nA_- \tag{18}$$

whereupon we may rewrite (13) as

$$\sigma = \frac{qB}{2T}\left\{c + \left[c^2 + 4A_+A_-\exp\left(-\frac{g_+^\circ + g_-^\circ}{kT}\right)\right]^{\frac{1}{2}}\right\}\exp\left(-\frac{U}{kT}\right), \tag{19}$$

and Equation (15) becomes

$$\sigma(\text{high temperature}) = qB(A_+A_-)^{\frac{1}{2}}\exp\left(-\frac{U + \left(\frac{g_+^\circ + g_-^\circ}{2}\right)}{kT}\right) \tag{20}$$

To find the value of c, we use the procedure outlined in chapter I; we determine T_k and then use the equation

$$c = (A_+A_-)^{\frac{1}{2}} \exp(-\frac{E}{2kT_k}) \qquad (21)$$

where E is found from the conductivity plot.

In order to determine the value of A_+A_-, however, more information is needed; a plot of σ vs. c, the impurity concentration will enable us to determine this value. Haven[15] determined A_+A_- for lithium fluoride; Dreyfus and Nowick[16] found it for sodium chloride.

CHAPTER III

THEORY OF CHARGED DISLOCATIONS

Surface Potentials of Crystals[17]

The mechanism for the formation of a Schottky vacancy in a crystal requires that the vacancy be formed at the surface and diffuse into the interior. If the energy of formation of one of the vacancy types exceeds that of the other, an excess of this type of vacancy will be formed at the surface. Let us say, as is usually the case in the alkali halides, that the cation formation energy is less than the anion vacancy formation energy. There then will be more positive ion vacancies emitted into the crystal from the surface than negative ion vacancies, and the surface of the crystal will be positively charged.

The positive charge on the surface produces an electrical potential which inhibits the further formation of cation vacancies and encourages the formation of anion vacancies. As we go into the crystal from outside, we find first the positively charged surface, and then a negative charge cloud extending into the crystal. This cloud is caused by the excess of positive ion vacancies emitted by the surface. Beyond the cloud, the crystal is electrically neutral; there are as many

cation as anion vacancies. Thus, due to the difference in the formation energies of the positive and negative ion vacancies and the ability of the surface to act as a source of vacancies, the surface of the crystal is charged, with a compensating charge cloud extending into the crystal.

Dislocation Core Potential

A dislocation can act as a source or sink of vacancies, in much the same manner as a surface. By analogy with the surface charge on a crystal surface, it is possible for the core of a dislocation to be charged; further, there will be a compensating charge cloud surrounding the dislocation. A potential difference will exist between the core and the part of the crystal that is far from the dislocation.[18]

If the average potential at any point of the crystal is denoted by $v(\bar{r})$, then the concentration of cation vacancies will be given by a Boltzmann factor,

$$\frac{n_+}{N} = \exp\left\{-\frac{g_+ - ev(\bar{r})}{kT}\right\} \tag{22}$$

Likewise, the concentration of negative ion vacancies is given by

$$\frac{n_-}{N} = \exp\left\{-\frac{g_- - ev(\bar{r})}{kT}\right\} \tag{23}$$

where $-ev(\bar{r})$ and $ev(\bar{r})$ is the energy in the crystal potential of a cation and an anion vacancy respectively.

At distances far from the surface and dislocations, the concentrations are

$$\frac{n_+^\infty}{N} = \exp -\left\{ \frac{g_+ - ev_\infty}{kT} \right\} \equiv \alpha, \tag{24}$$

$$\frac{n_-^\infty}{N} = \exp -\left\{ \frac{g_- + ev_\infty}{kT} \right\} \equiv \beta, \tag{25}$$

where v_∞ is the potential of the crystal far from surfaces and dislocations. In these regions the crystal is electrically neutral. If α is the concentration of cation vacancies, β is the concentration of anion vacancies, and c is the concentration of divalent cations, then we have as the electroneutrality condition

$$\alpha = \beta + c \quad . \tag{26}$$

Substituting for $\exp(-\frac{g_+}{kT})$ in Equation (22) gives

$$\frac{n_+}{N} = \frac{n_+^\infty}{N} \exp\left\{ \frac{e(v - v_\infty)}{kT} \right\} , \tag{27}$$

as the expression for the concentration of positive ion vacancies at position $\bar{r}$ in the crystal. On taking the logarithm of Equation (24), we get

$$\ell n \frac{n_+^\infty}{N} \equiv \ell n\alpha = -\frac{g_+}{kT} + \frac{ev_\infty}{kT} \quad . \tag{28}$$

Now $\exp(-\frac{g_+}{kT})$ would be the concentration of cation vacancies that would be expected if we had not taken the electroneutrality condition into account. Writing $\ell n\alpha'$ for $-g_+/kT$, we have

$$\ell n\alpha - \ell n\alpha' = \frac{ev_\infty}{kT} \quad , \tag{29}$$

To get an expression for α, combine Equation (24) and (25) to get

$$\alpha(\alpha - c) = \exp\left\{-\frac{g_+ + g_-}{kT}\right\} = x_0^2 \tag{30}$$

This will be recognized as Equation (11) of chapter II. The solution is

$$\alpha = \frac{c}{2}\left\{1 + \left[1 + \frac{4}{c^2}\exp\left\{-\frac{g_+ + g_-}{kT}\right\}\right]^{\frac{1}{2}}\right\} \tag{31}$$

As before, we note that at low temperatures $\ell n\alpha = \ell n\ c$; at high temperatures $\ell n\alpha = -(g_+ + g_-)/kT$. Thus the expression for $\ell n\alpha$ shows two distinct regions as a function of temperature; however, $\ell n\alpha'$ always has the value $-(g_+/kT)$. The function $(\ell n\alpha - \ell n\alpha')$ will then show maxima and minima as a function of temperature. In particular, if $\alpha = \alpha'$, the expression would vanish. If we know the temperature at which this occurs, it would be possible to calculate the formation energy for cation vacancies at that temperature. The temperature for which the function $(\ell n\alpha - \ell n\alpha')$ vanishes is known as the isoelectric temperature, T_c, from the analogy to the Deby-Huckel theory of strong electrolytes. At this temperature $v_\infty = 0$, the dislocation core is uncharged, and the charge cloud vanishes.

If we know T_c we may write

$$\ell n\alpha = \ell n\alpha' = - g_+/kT_c \ , \tag{32}$$

so that

$$g_+ = kT_c \ell n(\frac{1}{\alpha}) \ . \tag{33}$$

The value of α may be found from ionic conductivity measurements if we are dealing with alkali halides. Thus the properties of charged dislocations may be used in conjunction with ionic conductivity data to determine the individual formation energies of anion and cation energies in alkali halides.

CHAPTER IV

STATEMENT OF THE PROBLEM AND PREVIOUS WORK

Statement of the Problem

It has been seen that if the knee temperature of the conductivity plot of an alkali halide is known, the effective concentration of divalent cations present in the sample may be estimated. Further, by determination of the isoelectric temperature of the sample as well, the formation energy of individual ion vacancies can be estimated.

In this work, the problem was to construct equipment and collect data for the determination of these quantities for lithium fluoride. This choice was made because of the large amount of published material on the properties of dislocations in this substance; also, conductivity parameters were available with which certain portions of the work could be checked.

Review of Previous Work

Alkali Halides in General

The ionic conductivity of alkali halides has been widely studied. Kelting and Witt[4] showed that the presence of divalent impurities in potassium chloride enhances the conductivity in the extrinsic

region, the amount of conductivity increase being proportional to the amount of added impurity. Etzel and Maurer demonstrated the same for sodium chloride doped with calcium.[19] Much of the recent work in ionic conductivity is concerned with the study of the association of divalent cations and cation vacancies at lower temperatures; this is a subject that is beyond the scope of this thesis.

There are two effects that can contribute to the uncertainty in the experimentally determined value for the energy of vacancy pair formation in an alkali halide.[3] One uncertainty arises in the determination of the slope of the conductivity plot at lower temperatures, due to the association phenomena mentioned above. When sufficiently low temperatures are reached, the association removes some of the cation vacancies from participation in the conduction process. The conductivity plot is then concave toward the 1/kT axis, making it difficult to establish a true slope for the mobility activation energy. This introduces an uncertainty in the mobility value, and subsequently in the value of the vacancy pair formation energy.

The second uncertainty arises at high temperatures, where the anions contribute increasingly to the conduction. Since the activation energy for anion conduction is much higher than that for cation conduction, we need only consider it at high temperatures. On the conductivity plot, anion conduction causes the conductivity to be larger than it would otherwise be. Thus the plot is made convex towards the 1/kT axis, making an exact determination of the slope difficult.

Haven[20] showed that the form of the conductivity plot for lithium halides was consistent with the results of the theoretical development in Chapter II. By considering several alternative processes for the conductivity mechanism, and comparing the results obtained with the form of the conductivity plot in the region of the knee temperature, he showed that only Equation (30) of chapter III would adequately describe the curve in this region.

Lithium Fluoride

Haven[15] studied the ionic conductivity of crystals of lithium fluoride doped with magnesium. The conductivity parameters that he obtained have been widely used in LiF studies and will be used in this work. More recent data in this area would be desirable, but none are available. Haven found the values of the conductivity parameters for LiF to be

$$g_+^\circ + g_-^\circ = 2.68 \text{ eV.} \qquad A_+A_- = 2.5 \times 10^5$$

In the work reported in this thesis it was possible to establish the value of $g_+^\circ + g_-^\circ$, but Haven's value for A_+A_- will be used. In order to check the value of A_+A_- it would be necessary to study the conductivity of LiF as a function of the divalent cation concentration.

Charged Dislocations

After the work of Eshelby et al.,[18] in which it was predicted that dislocations in ionic crystals should be charged, a number of experiments were carried out to verify his predictions. The early studies of charge effects accompanying dislocation motion were centered around an indentation technique,[21] where charge was induced on electrodes by indenting the crystal surface with a diamond point. It was difficult to interpret these experiments, however, for it was not known whether the dislocations moving toward or away from the indentation point were the important ones.

Amelinckx, Vennik, and Remaut[22] arranged a crystal of NaCℓ so that it could be bent and straightened repeatedly in a sinusoidal manner. By painting electrodes on various faces of the crystal, they observed electrical effects accompanying the application of the repetitive stress. It was found that a potential difference was developed between the tension and compression faces and the ends of the crystal. This potential difference had the same frequency as the applied stress. A phase lag was present, however; it was ascribed to the time lag between the initial application of the stress and the achievement of the critical stress necessary to initiate plastic flow. It was noted that:

1) Signals on both the compression and the tension side were in phase.
2) The wave shape was typically flat-topped in the frequency range 10-10,000 hz.

3) The signal increases in amplitude with increasing plastic bending.

4) The signal from the crystal is observed only if the stress exceeds a certain critical value. The electrical signal then grows very rapidly in amplitude and is a nonlinear function of stress.

5) The signal decays in amplitude with continued stressing.

These authors also presented a strong argument against the electrical signal being due to a piezoelectric type effect. In addition, they found that the charge on the dislocation core was positive at room temperature.

In a later paper, Remaut and Vennik[23] reported on a different method of observing the electrical signal. The specimen to be tested was first bent in a four point bending jig so as to induce pure bending in the center section of the crystal. This induced an excess of dislocations of one mechanical sign into the crystal. The specimen was then mounted in a device that subjected it to a push-pull stress (alternate compression and extension). It was found that the signals were out of phase on the tension and compression faces, exactly as expected. Some interesting photographs of oscilloscope traces of these signals are contained in References (22-23).

Caffyn and Goodfellow[24] cleaved a slab of NaCl crystal into two halves along the long axis and parallel to the tension and compression faces. They then rejoined the halves with a conducting cement.

Using the cement as one electrode, they studied the potentials developed during the four point bending of a NaCℓ sample having electrodes painted at various places on its surface with silver paint. They were very careful to take into account the various modes of bending of the rock-salt structure. It was found that the center of the sample was always negative with respect to the tension and compression faces, as long as the electrode was far away from the position where the knife edge contacted the surface. In addition, they observed the intense birefringence due to the excess of dislocations of one mechanical sign located near the neutral axis. This gave further assurance that such a concentration of dislocations actually occurs. Caffyn and Goodfellow concluded that the dislocations carry a positive charge at room temperature.

Hikata et al.[12] studied in detail the potentials associated with plastic deformation of NaCℓ and found agreement with most prior work. They concluded that the screw segment of a dislocation was not charged, and that the edge component carried a positive charge at room temperature. They subjected samples to bending deformation and to tensile and compressive stresses. The modes of bending of the rocksalt structure were taken into account, and effects associated with the various bending modes were discussed. In addition, extra dislocations were introduced at the surface of the crystal and their effects on the electrical signal were examined.

Davidge[25] discussed at some length the application of the theory of Bruneau and Pratt[11] concerning the bending of crystals having the rocksalt structure. He also concluded that the screw segments of dislocations are not charged, in agreement with Hikata et al.[12] He demonstrated that if one wants to obtain unambiguous results from pre-bent crystals, it is necessary to have the crystal bent predominantly in the two dimensional mode. If the crystal is deformed in three dimensional bending, the sign of the electrical effect can actually change between two adjacent electrodes on the same face of a crystal. Davidge determined that dislocations in a nominally pure sample of NaCℓ carry a negative charge, while dislocations in a sample of NaCℓ doped with Na_2O_2 carry a positive charge. Davidge hypothesized that in the latter case a "pseudo-intrinsic" region existed because of association between the cation and anion impurity ions.

In a later paper, Davidge[26] carried out an experiment where the variation of the electrical effect was studied as a function of temperature. Three samples of varying impurity content were used; after pre-bending, they were inserted into a push-pull deformation apparatus. By using the results of Dreyfus and Nowick[16] for the relevant conductivity parameters, he determined the effective concentration of divalent cations in his samples and the concentration of positive ion vacancies as a function of temperature. He found that the dislocations in NaCℓ are negatively charged below the isoelectric temperature; above this temperature, they are positively charged. The isoelectric

temperature found for the samples ranged from 400°C to 500°C. He calculated the energy of positive ion vacancy formation to be (0.95 ± 0.10) eV at 0°K.

Strumane and De Batist[27] also studied the variation of the electrical signal from NaCℓ with temperature. They found that the electrical signal changed sign twice between room temperature and 800°C. By using an expression for the dislocation line charge derived earlier, they determined the value of g_+° to be (0.93 ± 0.09)eV. This is in excellent agreement with the value obtained by Davidge.

Schwensfeir and Elbaum[28] have established the existence of an isoelectric temperature in NaCℓ by direct observation of the motion of grain boundaries under applied electric fields at elevated temperatures. They used bicrystals with a grain boundary of ∿1° misorientation. For one of their specimens, the boundary motion indicated that it had a negative charge at 560°C ; at 640°C , however, the motion indicated that it was positively charged.

Kliewer and Koehler[29] studied the thermal properties of charged dislocations using an internal friction technique. The procedure was to determine the value of Young's modulus and the damping factor for ultrasonic waves sent through NaCℓ samples at high temperatures. By extrapolating their results for g_+ to absolute zero, they found a valve for g_+° that overlapped that of Davidge. They further found that the condition $g_+ < g_-$ for NaCℓ is essentially due to the temperature dependent terms in the formation free energies.

Most of the work on charged dislocations has been carried out with NaCℓ. Some authors have examined KCℓ, but their results are of an indirect nature.[30] Sproull[31] carried out a set of measurements in which he attempted to determine the value of g_+° for lithium fluoride. He bent a crystal by heating it and then forcing it into a notch cut in a plate, thus causing a v-shaped bend of 55° in the crystal. One end of the crystal was then fixed and the region of the bend was subjected to a strong electric field. The resulting motion of the free end was measured. Although there seems to be no doubt that a motion of the free end was detected, the uncertainty in measuring displacements of the order of angstrom units probably leads to incorrect results. In addition, the mode of bending of the crystal was probably a mixture of the two-dimensional and the three-dimensional types. Since the two-dimensional type of bending is the type that gives unambiguous results, the presence of three-dimensional bending probably caused inconsistencies. Sproull gave $g_+ = 0.3$ eV, but mentioned that his value seemed unreasonably low.

CHAPTER V

EXPERIMENTAL METHODS

Ionic Conductivity Measurements on Lithium Fluoride

Introduction

The ionic conductivity measurement was made to find the concentration of cation vacancies as a function of temperature. The relationship between the ionic conductivity and the geometrical parameters of the measuring systems is given by

$$\sigma = \frac{L}{A} \cdot \frac{1}{R} \tag{34}$$

where σ = conductivity

L = length of the current path

A = area of the electrodes

R = resistance between the electrodes.

Equipment and Sample Preparation

The conductivity of lithium fluoride was determined from the resistance and dimensions of a circular sample with its faces parallel to (100) planes. The samples were cut from cylindrical specimens by

means of a wire saw, using a glycerine-water-600 mesh carborundum slurry. The resulting discs were then carefully ground with 250 mesh carborundum to give parallel faces. The sample width was measured with a micrometer just prior to applying the electrodes, which were formed by painting Dag dispersion 154, a suspension of colloidal graphite in acetone, onto the crystal surface. Etzel and Maurer,[19] in their experiments on NaCℓ found no conductivity difference between electrodes of graphite and electrodes of evaporated platinum; however, they noted a tendency for the platinum to evaporate at high temperatures. Since the melting point of LiF is 41°C higher than that of NaCℓ, and the measurements were expected to take 7-15 days, the colloidal graphite was chosen in order to prevent deterioration of the electrodes.

A circular electrode of diameter ½ inch was painted onto one face of the crystal such that it coincided with the center of the crystal. An annular guard ring was painted on the same side of the crystal, while the other side was covered totally so as to form a single electrode. The guard ring was included because of the possibility that surface currents might cause an incorrect value of resistance to be registered; by maintaining this electrode at the same potential as that of the center electrode, no current could occur along the surface to the center electrode.

The largest source of error in Equation (34) is in the area of the electrodes. The geometrical error can be made very small, but the

percentage of the area which actually contributes to the conductivity has been taken as much as 5 per cent uncertain in earlier work.[15] There is reason to believe that this uncertainty in our case is much smaller than this, which will be discussed later.

The contacts by which the crystal electrodes were connected to leads, were machined from pyrolytic carbon. Pyrolytic carbon has a low oxygen content, which allows it to be used at high temperatures without bulk decomposition. The contacts were made relatively massive so that their temperature would not be greatly influenced by temperature fluctuations in the surroundings. The guard ring was also made of pyrolytic carbon, and was insulated from the center electrode by a boron nitride ring. The lower contact had an insulated chromel-alumel thermocouple embeded in it, only a few millimeters from the lower surface of the crystal. The size of the contacts and the placement of the thermocouple allowed a precise knowledge of the crystal temperature.

The center contact-guard ring assembly was spring loaded so as to maintain a constant pressure on the crystal. A platinum disc was placed between the lower electrode and its contact to ensure a good connection; thus the only materials in contact with the crystal were carbon and platinum. The crystal contact assembly is shown in Figure 9.

The sample tube was surrounded by a quartz tube with aluminum end pieces. The electrical connections were made through these end pieces, which were well away from the high temperature region. A furnace having chromel heater wire and asbestos insulation was placed around the quartz tube; no temperature controller was used, but a

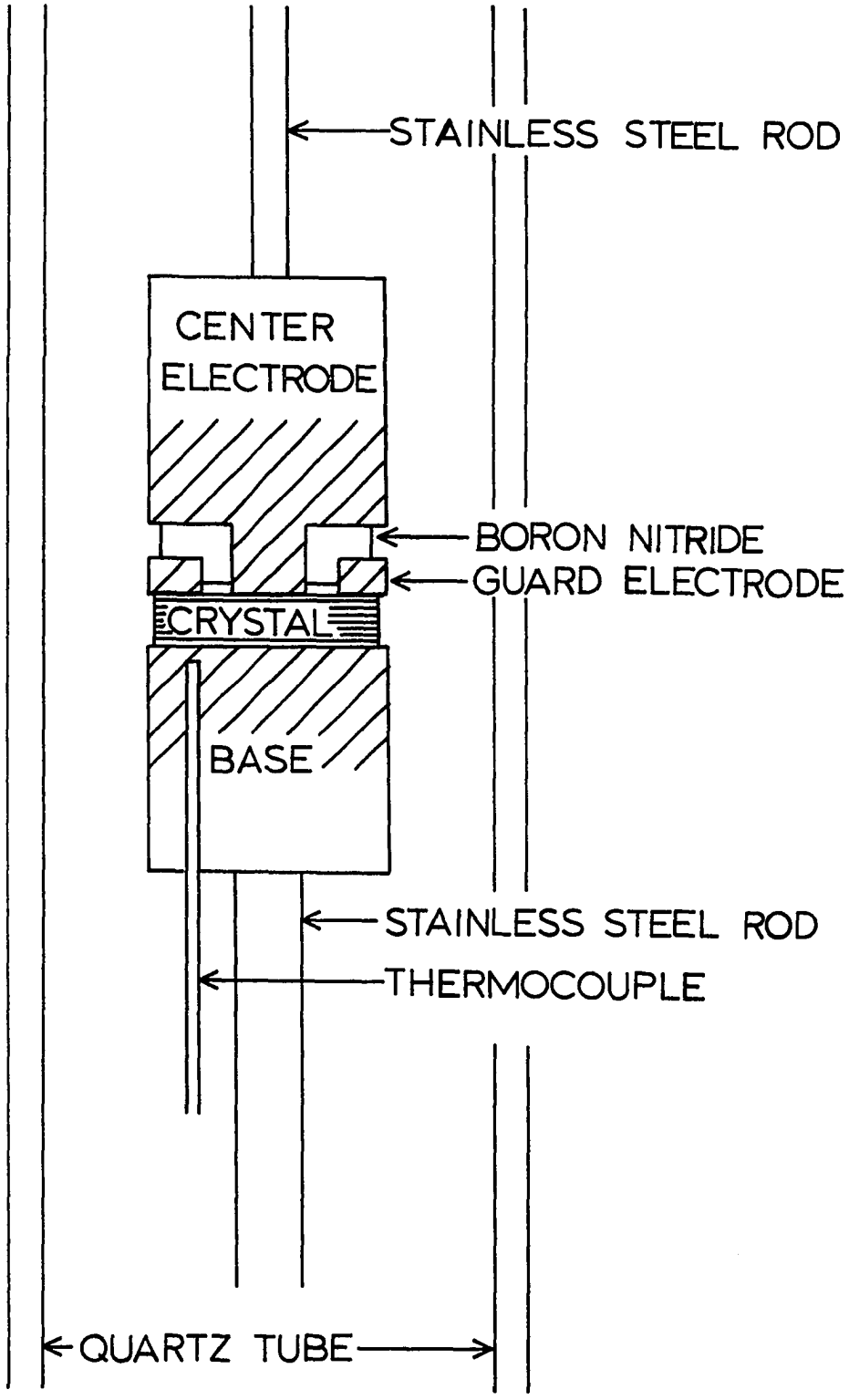

FIGURE 9. IONIC CONDUCTIVITY APPARATUS

voltage regulator provided constant voltage for the autotransformer that was used to control the furnace current. This prevented line voltage fluctuations from changing the furnace temperature.

To further protect the crystal electrodes, as well as the carbon contacts, a flow of dry nitrogen which had been filtered through a molecular sieve trap was passed through the tube. The pressure of the nitrogen was kept slightly above atmospheric.

When the initial conductivity data was analyzed, the conductivity of different crystals differed by as much as a factor of 5 even in the intrinsic region. The reason for the variation was found to be a miscalculation of the center electrode area. The electrode was always painted larger than the contact, which was a ½ inch diameter circle. At high temperatures, the part of the electrode not directly under the contact would separate from the crystal surface. When the data was recalculated on the premise of a ½ inch diameter electrode, the intrinsic conductivity for the three crystals agreed within experimental error. A special step in preparing a sample for conductivity measurements, called the "setting-in" process, was instituted in order to obtain reproducible results. It is described in the next section.

Measurement Procedure

After closing the system and flushing it with nitrogen, power was applied to the furnace. The nitrogen flow was then reduced to a low value and the temperature was allowed to rise to 800°C in order to set the size of the electrodes with respect to the crystal, as mentioned in the last section. The high temperature allowed the lithium

fluoride to undergo any plastic deformation or relaxation that might occur before measurements were started. The temperature was allowed to remain at 800°C overnight.

An ordinary Wheatstone bridge was used to measure the resistance of the crystal; alternating current of frequency 500 hz was used as the power source. A variable capacitor was shunted across the Wheatstone bridge so that a satisfactory null could be achieved with the D.C. bridge. The null point was detected by using a General Radio null detector type 1232A. This arrangement could be used from 350°C to the melting point of lithium fluoride, corresponding to a resistance range of 10^7-10^1 ohms. At low temperatures the null was shallow and tended to be disturbed easily by outside influences, while at high temperatures the low resistances caused severe loading of the voltage source.

It was necessary to use the alternating voltage source to avoid ambiguity in the value of the conductivity. In a direct current conductivity measurement, the resistance varies with the amount of charge that passes through the sample. A number of explanations have been offered for this phenomenon,[32-34] but usually it is simply avoided by using an alternating current source.

The guard ring was connected through a separate decade resistance box to the voltage source. Its resistance was kept at the same value as the main dial of the Wheatstone bridge. The null was taken, then, with the guard ring at the same potential as the center electrode,

while only the center electrode was effective in the conductivity measurement. At low temperatures the guard ring potential did not affect the null point, while there was a marked effect at high temperatures. It was not determined whether the effect was due to surface conduction or to the geometry of the electrodes. No significant phase difference between the guard ring and the center electrode was apparent, for even at high temperatures the null could be reduced to the level of the noise in the circuit.

The system was allowed two hours to stabilize after changing the current in the furnace coils. At the end of this period of time, a 15 minute check was run on the temperature; if less than 1 °C variation was detected in this time, the conductivity was measured. If the temperature varied by more than 1 °C. in this period, an additional wait of 30 minutes was made and the procedure repeated. Temperature drifts were especially bad in the high temperature region prior to the installation of the constant voltage transformer.

Push-pull Deformation Experiment

Equipment

The final design for the push-pull deformation apparatus is shown in Figure 10; with this design, a cyclic compressive-tensile stress could be applied to the sample. The crystal is mounted between two anvils, one rigidly fixed and the other movable. The anvils were made of stainless steel rod; for rigidity the fixed anvil was firmly bolted to a 70 pound slab of ½ inch Inconel metal plate. The crystal

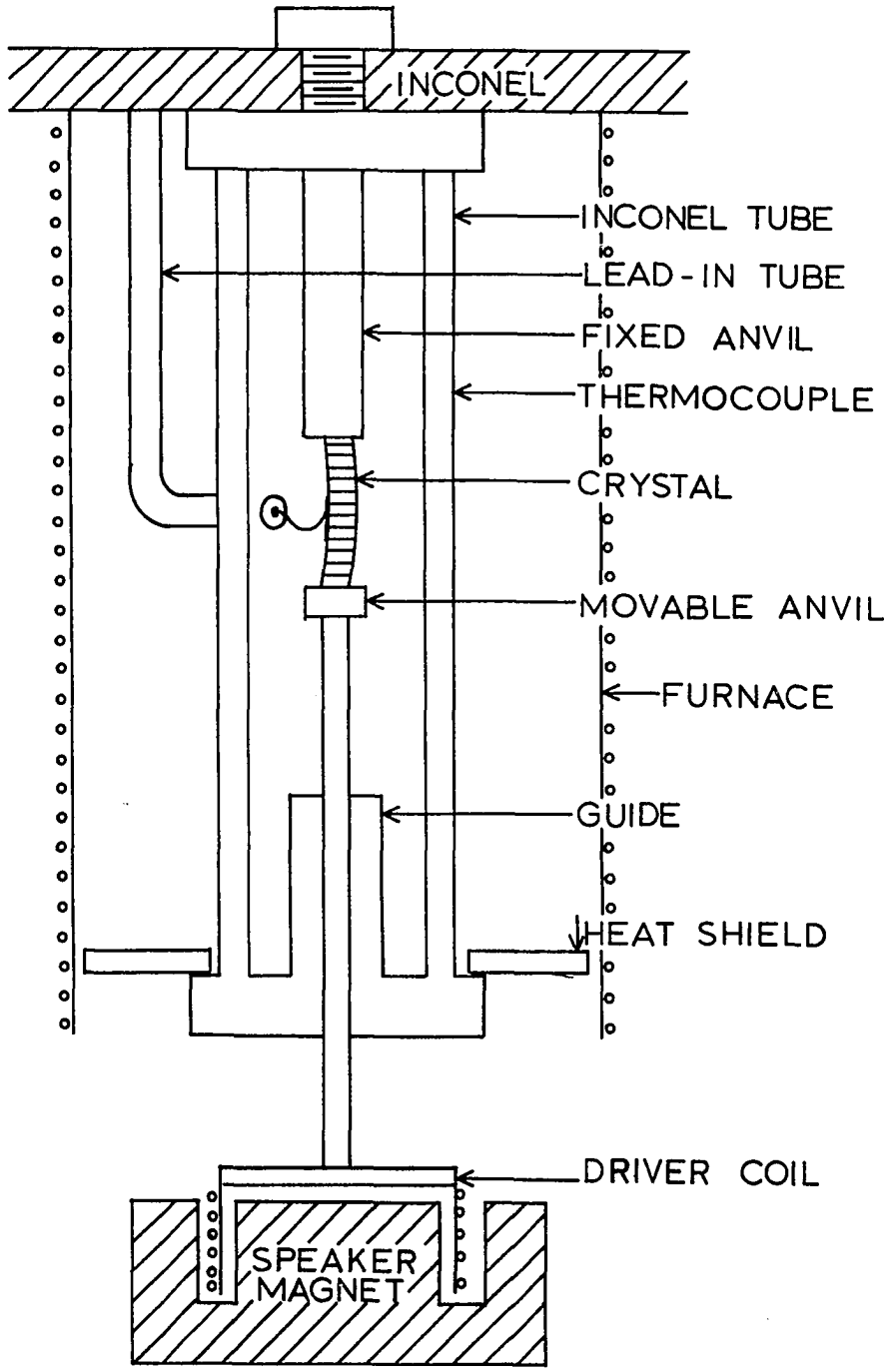

FIGURE 10. PUSH-PULL DEFORMATION APPARATUS

under test was cemented to the two anvils using Sauereisen high temperature cement. The movable anvil passed through the stainless steel end cap of the sample chamber; outside, it was connected to a coil wound on a nylon form. The coil was inserted in the field of a loudspeaker magnet. By passing an a.c. current through the coil, a push-pull type stress could be applied to the crystal.

The sample chamber was a tube of Inconel in which a window was cut to make the crystal accessible. Stainless steel end pieces capped the Inconel tube and added to its rigidity. Quartz insulated chromel wire, cemented into a stainless steel tube served as a high temperature lead-in. The upper end of the lead-in was terminated in a teflon insulated BNC connector, thus entirely shielding the center wire. The sample chamber and the lead-in tubulation were fixed to the Inconel slab separately to minimize the mechanical vibration of the system. The slightest relative motion of parts that were in proximity to either the crystal or to the center lead-in wire resulted in spurious electric signals being generated. The crystal signal source impedance was so high that such extra signals were intolerable.

The entire assembly was mounted on a framework made of $1\frac{1}{2}$ inch angle iron. A shelf, made of $\frac{1}{2}$ inch aluminum sheet, was installed in the framework; the magnet was positioned on it.

The magnet coil was driven by a 40 watt Altec-Lansing high fidelity amplifier. The amplifier was fed from a Hewlett Packard audio oscillator, model 200CD, with a 600 ohm output impedance; there

was little difficulty in feeding directly into the high impedance of the power amplifier. With this arrangement the crystal was driven at frequencies of 10-100 hz, although usually at 200 hz. Above 1000 hz. the coil and linkage arrangement was too heavy to respond to the driving signal.

From the lead-in, the crystal signal was introduced into a type 5800 electrometer tetrode vacuum tube. This tube has a nominal grid leakage of 10^{-15} amperes, thus allowing very high input impedances. The power for this tube was obtained wholly from mercury batteries, so that no a.c. hum would be introduced through the power source. The electrometer circuit as shown in Figure 11 has a gain of approximately unity, but the output impedance is about a megohm. Since the grid resistor of the tetrode electrometer is 2×10^{11} ohms, this arrangement provided a good impedance match. The electrometer output was fed into an ordinary audio amplifier with provisions for low level signals. The filaments of the amplifier tubes were supplied with direct current to eliminate hum. High voltage was taken from an electronically regulated power supply; at 250 volts, the voltage gain of the electrometer-audio amplifier complex was 1500.

A Tektronix double beam oscilloscope, type 502, was used to display the signal from the amplifier. One channel was used to display the electrical signal from the crystal, and the other showed the signal from the audio oscillator. In this manner the phases of the electrical signal from the crystal and the input signal could be compared. The oscilloscope was equipped to take photographs of the traces,

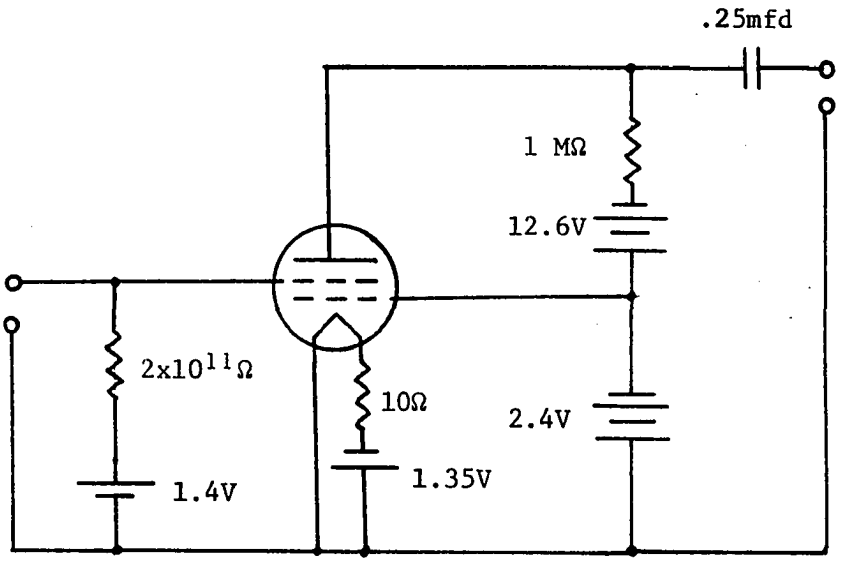

Figure 11. Electrometer Circuit

thus allowing a pictorial record of the null point corresponding to the isoelectric temperature.

A great deal of care was taken in preparing the samples for the push-pull deformation experiment. The lithium fluoride was obtained from the Harshaw Chemical Company in the form of three cylinders, each 1½ inches long and 1 inch in diameter. One end of the cylinders was cut off and used as the ionic conductivity sample; the remaining part was cut into slabs to be used in the deformation apparatus. The high purity of the specimens made it impossible to cleave them; instead, it was necessary to cut the samples using a wire saw and a carborundum slurry. Rather than cleave along the (100) planes, the samples would either deform plastically or facture at the point where the cleaving was attempted. Usually a fracture of the crystal along a (110) plane would occur. This difficulty in handling highly pure LiF is also mentioned in the literature.[9,35] The final procedure adopted in handling the samples is as follows: 1) Locate the cleavage planes by observing surface scratches with a microscope. 2) Mark the edge of the cleavage plane as it intersects the end of the cylinder. 3) Place the edge of the cleaving knife parallel to the axis of the cylinder, pointing inward along a diameter bisecting the angle between (100)planes. 4) Tap the cleaving knife gently with a small hammer, near one end of the cylinder. This last step usually starts two perpendicular cleavage planes a small distance into the crystal. Using these planes as guides, the crystal was set up in the crystal saw with

the wire blade approximately parallel to the (100) planes. The slab was then cut from the main crystal and checked for parallelism. If the surfaces were not parallel, they were ground with 250 mesh carborundum powder until they were within .001" of being parallel. All marks of the first grinding were then removed by grinding with 600 mesh carborundum. A third grinding with 1000 mesh carborundum was then carried out, continually rotating the crystal so as to grind the surface evenly. After about 30 minutes of this final grinding, the crystal surfaces were usually less than .0005" from being parallel. This last step probably brings the surface very near to a (100) plane. The final thickness of the crystal was approximately .07". The crystal was annealed for 40 hours following the final grinding to remove as many grinding faults as possible.

Two bending jigs were made, each consisting of equally spaced dulled knife edges. The geometry and dimensions of these jigs are shown in Figure 12. They were used to introduce an excess of dislocations of one mechanical sign into the crystals. The procedure used in bending a crystal is as follows: the crystal surface was lubricated with a silicone grease to minimize any friction between the knife edges and the crystal. The crystal was then positioned in the jig; stress was applied by pouring sand into a plastic container placed on the top die. A dial indicator was used to show the deflection of the top die with respect to the bottom die. Several catastrophic failures were caused by adding sand too quickly to the container; the successful bends usually took 4-9 hours to complete. In the later stages of

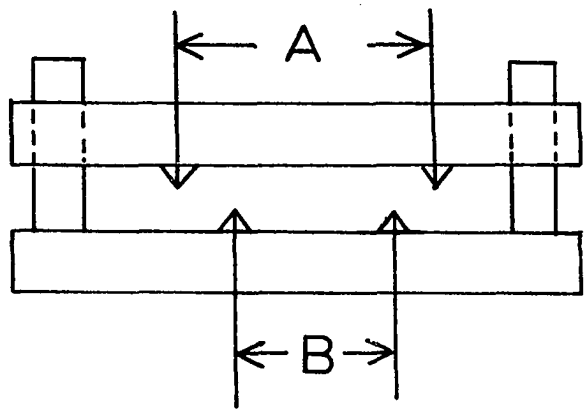

JIG	DIMENSION A	DIMENSION B
1.	0.750"	0.4"
2.	1.125"	0.7"

Figure 12. Bending Jigs

the experiment, the crystal was allowed to reach its final configuration by steady creep. This resulted in considerably fewer broken crystals, but the preparation time was approximately doubled. Smaller signal strength was encountered in the samples deformed by creep than in those deformed dynamically, probably due to fewer dislocations.

After bending the crystal, it was installed in the apparatus as already mentioned. Silver electrodes were painted on the crystal, and the connection from the lead-in to the electrode was made by a length of .004" diameter platinum wire. Two silver paints were used; a water base type SCP-14 for the crystals proper, and an organic base type SC-14 for fastening the platinum wire to the electrode thus formed. Both types were made by the Micro-circuits Corporation.

After installing the crystal in the Inconel tube, the signal from it was examined. The phase and amplitude of the room temperature signal was recorded. Power was then applied to the furnace coils, and a small amplitude stress is applied to the crystal. Continuous observation of the signal was thought unnecessary, since any changes occuring with temperature were very slow. The isoelectric temperature was detected as a 180° phase change in the crystal signal, since the minute nature of the signals made observation of a null point difficult. Sharp values for the isoelectric temperature were virtually impossible, since it appeared that the temperature might be a function of the stress amplitude. The best results were obtained when the signal was run at a barely detectable level, for the stress was very small in that

case. This difficulty in observing the isoelectric temperature was also noted by Strumane and De Batist[27] in their work on NaCℓ. Conclusions about the shape, magnitude, and phase of the signal from lithium fluoride parallel very closely their observations.

The temperature was allowed to increase some 50°C above the isoelectric temperature to determine if the crystal signal would continue to grow in amplitude. The temperature was then swept through the isoelectric temperature phase change several times, each time more slowly. In this way the true isoelectric temperature was bracketed; the effective isoelectric temperature was taken as the center temperature of the bracket.

After lowering to room temperature, the signal strength was found to be weaker than before, but still easily detectable. In one case, the signal strength was actually greater than before. Upon examination, it was found that cleavage cracks had occurred in the neighborhood of the electrodes. In this crystal, the isoelectric temperature had been very hard to locate.

CHAPTER VI

RESULTS AND DISCUSSION

Ionic Conductivity

The ionic conductivity equipment worked well from the beginning, although reproducible results were hard to obtain until the setting-in procedure was adopted. Low signal strengths at low temperatures, due to the high crystal resistance, was the only difficulty encountered in taking data. The conductivity plots of the three LiF samples are shown in Fig. 13. A least squares method was used to find the transition temperature, T_k; the data from each crystal was separated into two temperature regions, with data from the temperature range around T_k discarded. Thus, for a given crystal, one data set correspond to the intrinsic region and the other to the extrinsic region. By assuming that in both regions the data fitted an equation of the type

$$\ell n\sigma = A + B \frac{10^3}{T} \quad , \tag{35}$$

A and B for each region was determined by least squares analysis, and are given in Table 1. The two expressions for a given crystal were equated to each other and solved to determine T_k.

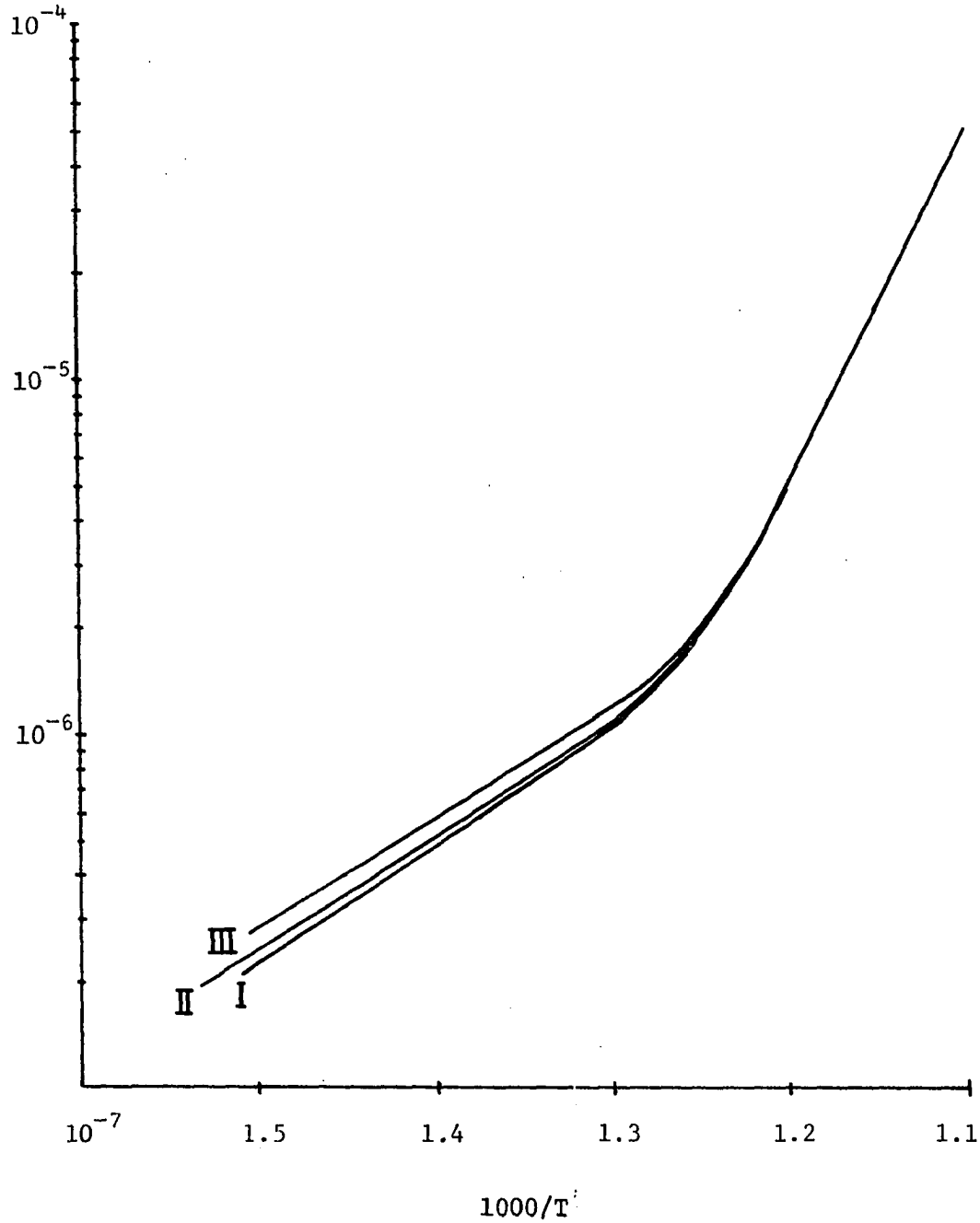

Figure 13. Conductivity plots

Even though the conductivity plot for a crystal is defined to be $\ell n\sigma T$ vs. 1/T, we have plotted $\ell n\sigma$ vs. 1/T in Fig.13 and have assumed that $\ell n\sigma = A + B\frac{10^3}{T}$ for the least squares fit. This is valid since T only varies from 250 °C to 800 °C in the temperature range of interest, while σ varies over several orders of magnitude. Thus ℓn T is effectively a constant with respect to $\ell n\sigma$, and is included in the constant A for convenience.

The value of T_k, along with the corresponding value for E, was used to determine the impurity concentration through the expression

$$c = (A_+A_-)^{\frac{1}{2}} \exp(-E/2kT_k) \quad . \tag{36}$$

The values of E, T_k, and c for our samples are shown in Table 1.

Push-Pull Deformation Experiment

The measurement of the isoelectric temperature was made difficult by the dependence of the phase change on the stress amplitude; near the isoelectric temperature T_c, the phase change could be encouraged by applying a large stress amplitude to the crystal. If the stress was large enough to cause plastic flow, the dislocations could sample their environment as mentioned by Strumane and De Batist,[27] thus leading to equilibrium faster than would occur with only diffusion processes occuring. Thus, if the isoelectric temperature had been passed but the crystal had not attained thermal equilibrium, the application of sufficient stress would cause an abrupt change of phase of the signal without passing through a null point.

Table 1. Least Squares Analysis

SAMPLE	EXTRINSIC REGION		INTRINSIC REGION		T_k
	A	B	A	B	
I	-2.988	-8.308	15.557	-23.041	794 °K
II	-3.684	-7.748	15.064	-22.711	798 °K
III	-3.252	-7.765	14.019	-21.619	802 °K

Sample	U (Mobility Activation Energy)	E	c
I	0.72 eV	2.54 eV	4×10^{-6}
II	0.67 eV	2.58 eV	3×10^{-6}
III	0.67 eV	2.38 eV	1.6×10^{-5}

The push-pull deformation equipment gave very little trouble after the initial design errors were corrected. The reproducibility of the isoelectric temperature of a given sample is quite good; some samples were tested again a week later with no appreciable change in the results. There is no doubt concerning the existence of a phase reversal but the determination of the exact null point is quite difficult.

The lack of sharpness could have been due to a number of factors; the rate of temperature change may have been a factor in the observed variation. Since the thermocouple is embedded in a stainless steel rod, there may have been a thermal lag between it and the crystal. It is also possible that the impurities were distributed inhomogeneously throughout the samples; different regions of the crystal would then have had different isoelectric temperatures. This would cause the "collective" isoelectric temperature to occur over a range, making a sharp determination of T_c impossible.

One way of possibly locating T_c, even without a sharp null value, would be to plot signal strength vs. temperature; it then would be possible to extrapolate to zero signal. A number of reasons make such a plot meaningless. When the crystal is pre-bent, as it must be in order to observe a signal, a compressive stress applied to its ends will further bend the crystal. Thus it is possible to create more dislocations of the correct mechanical sign by a compressive stress, leading to a signal enhancement. This has probably occured during these experiments. In addition, the number of dislocations actually contributing to the electrical

signal is undoubtedly a function of temperature. Above the isoelectric temperature, the signal is quite strong; below, it is weaker in general. The crystal was quite soft after an experiment and would bend quite easily, indicating that dislocations may have been worked out of the crystal at high temperatures. A plot of signal strength vs. temperature was tried for several samples, but the signal strength variation was of the same order as the signal itself.

The use of a phase sensitive amplifier is a possibility for detecting the phase change. Very slow temperature changes would have to be used with this approach because of the high level of filtering necessary when dealing with low signal strengths.

The values of T_c are given in Table 2. As mentioned earlier, the effective value is taken as the center temperature of the bracket formed by T_c found with increasing temperature and T_c found with decreasing temperature.

If now the values of T_c from Table 2 are put into the equation

$$g_+ = kT_c \ln 1/c \quad , \tag{37}$$

(where we use $\alpha = c$ since at 410 °C we are well within the extrinsic range), the values of g_+ for the samples are

$$g_+^I = 0.73 \text{ eV}, \qquad g_+^{II} = 0.74 \text{ eV}, \quad \text{and} \quad g_+^{III} = 0.73 \text{ eV}.$$

These values represent the cation vacancy formation energy at temperature T_c.

Table 2. Values of $g_+(T_c)$

SAMPLE	T_c	T_c(eff.)	$g_+(T_c)$
I	408°C - 413°C	407°C	
	402°C - 407°C	680°K	0.73 eV
	395°C - 408°C		
II	404°C - 412°C	408°C	
		681°K	0.74 eV
III	382°C - 392°C	390°C	
	388°C - 400°C	663°K	0.74 eV
	386°C - 397°C		

Conclusions and Discussion

LiF Experiments

These experiments have found a value of T_c, from which a value of g_+ at T_c can be calculated, using a simple theory. It is possible that the value of g_+ for a dislocation is different from g_+ for a surface; however, if we assume that $g_+(\text{dislocation}) = g_+(\text{surface})$, we can attempt to calculate $g_-(T_c)$. For lack of a more recent determination, we will use Haven's value of $(A_+A_-)^{\frac{1}{2}} = 500$;[15] the value of $(g_+ + g_-)_{T=0}$ will be the one determined from our measurements of the intrinsic slope, $(g_+^\circ + g_-^\circ) = 2.56$ eV. Thus we may write, using Equations (13) and (14) of Chapter II:

$$(g_+ + g_-)_{T_c} = (g_+ + g_-)_{T=0} = kT_c \ell n A_+A_- \quad ,$$

from which we find $(g_+ + g_-)_{T_c} = 1.84$ eV. Then, using the assumption mentioned above, since $g_+(T_c) = 0.73$ eV.,

$$g_-(T_c) = 1.10 \text{ eV.}$$

This result should be examined closely. Haven found the value of A_+A_- by plotting the experimental exponential factor of the conductivity plot in the extrinsic region (qBc of Equation (10), Chapter III) vs. c, so that the slope of the curve gave qB. He then divided the preexponential factor of the intrinsic region by qB, obtaining $(A_+A_-)^{\frac{1}{2}} = 500$ for LiF. He found the values of c for his samples by using a volumetric

analysis technique on the very crystals that he tested. Thus the value of A_+A_- found by Haven is subject to error from both the intrinsic and extrinsic pre-exponential factors, as well as from any inaccuracies that might have occured in the impurity determination. The actual error in Haven's A_+A_- is not stated, and new work needs to be done to refine the value of this parameter.

The theory used in analyzing the data presented here neglects several effects, among which are vacancy and impurity association, and anionic conduction at high temperature. Even the simplest extension of the theory requires additional parameters not necessary in the elementary treatment; for example, the Debye shielding radius of a dislocation, itself a function of g_+, is needed if the long-range coulomb effect between vacancies and impurity atoms is considered. We are dealing with a smoothed out theory, in which the details of dislocation charging, etc., is ignored. In fact, the cation vacancy concentration in the highly strained crystals used for the push-pull experiments might be different from that of the crystals used for ionic conductivity studies; Kanzaki et al.[36] have shown that a high dislocation density leads to an enhanced conductivity for high purity KCℓ and to a decreased conductivity for doped KCℓ, thus indicating that the state of strain of a sample might indeed be an important factor.

There is only one other experimental value of g_+ available; Sproull found $g_+ = 0.3$ eV. This result is unreasonably low, and Sproull concluded that association of vacancies and precipitation of impurities had affected his analysis, although as mentioned earlier,

his samples may have contained a large amount of two-dimensional bendings. In our experiment we have variations of ±7 °C in the value for T_c. From Equation (3) we have

$$\frac{\Delta g_+}{g_+} = \frac{\Delta T_c}{T_c} \tag{38}$$

so that we may have an error of 1 per cent in the stated value of g_+ due to the variation in the values for T_c. A further error can arise from an incorrect determination of T_k in the conductivity plot. The error in c caused by error in T_k is, from Equation (2),

$$\frac{\Delta c}{c} = \frac{E}{2kT_k} \frac{\Delta T_k}{T_k} \tag{39}$$

If the straight regions of the conductivity plot of a sample is extended to determine T_k, one can easily make an error of 2 per cent. Using Equation (5), one finds $\Delta c/c = 0.5$; by further assuming that $\frac{\Delta T_c}{\Delta c} \simeq 0$, we may write from Equation (3),

$$\frac{\Delta g_+}{g_+} = \frac{\Delta c}{c \ell nc} \tag{40}$$

Using $c = 10^{-5}$, $\Delta c = 0.5c$, we have

$$\Delta g_+/g_+ \simeq .05$$

An erroneous value of T_k then does not influence greatly the calculated value of g_+ using our simple theory.

NaCℓ Experiments

In order to check the validity of the results presented here for LiF, we tested two samples of NaCℓ in the same manner. One sample was from the Harshaw Chemical Company, while the other was home-grown from AR grade material. NaCℓ has been studied by several investigators[26,27,29], and their experimental procedures were discussed earlier. Kliewer and Koehler (KK) used an internal friction method,[29] while Strumane and De Batist (SD)[27] and Davidge (DA)[26] used essentially the the method employed in this work.

The conductivity data for the two samples are shown in Table 3. We have also entered T_c and the calculated value of $g_+(T_c)$ in this table. The formation energies calculated from the slopes of the straight line portions of the conductivity plots agree within experimental error with the literature values. These results were obtained using the same calculational procedure as for LiF. Even though our experimental procedure was essentially that of Strumane and De Batist and Davidge, the data that we obtained seemed to fit that of Kliewer and Koehler more closely. To illustrate we have plotted $\ell n(1/c)$ vs. $1/T_c$ taking care that $T_c < T_k$ for all samples so that the approximation $\alpha = c$ can be used. Since

$$g_+(T_c) = kT_c \ell n\left(\frac{1}{c}\right) = g_+^\circ - kT_c \ell n A_+ \qquad (41)$$

this plot will have g_+°/k as its slope.

Even though the point representing the Harshaw crystal is directly on the extension of line KK, the second point lies between

Table 3. Data for NaCℓ Crystals

Crystal	U	E	T_k	C	T_c
A. Harshaw	0.7 eV	2.01 eV	729 °K	1.3×10^{-6}	627°K
B. Home-grown	0.94 eV	2.10 eV	879 °K	1.7×10^{-5}	761°K
C. Dreyfus and Nowick[16]	0.80 eV ± .03 eV	2.12 eV	-	-	-

the lines KK and DA. The slopes of both lines are almost equal, thus yielding nearly the same value of g_+°. Using the simple theory in which association and precipitation is ignored, Kliewer and Koehler found $g_+^\circ = 1.4$ eV, while the Davidge data DA as plotted in Fig. 14 yields $g_+^\circ = 0.85$ eV. Davidge's actual result was $g_+^\circ = 0.95 \pm 0.1$ eV; his values of T_c were so close to T_k that the simple approximation $\alpha = c$ could not be used. It is interesting to note that his stated experimental result does overlap the value obtained using this approximation, however.

Using our data points and that of Strumane and De Batist, we find that $g_+^\circ = 0.8$ eV. Although no error analysis was carried out for the NaCℓ data, this value is close enough to that of previous investigators to allow us to conclude that our procedure yields physically significant data. The value of g_+ obtained for LiF is then probably reliable.

The data can also be plotted in the form of $T_c \ell n(\frac{1}{\alpha})$ vs. T_c to give a straight line of slope $\ell n A_+$. In this way Davidge finds $A_+ = 7.6$, while in the same approximation Kliewer and Koehler obtain $\ell n A_+ = 12$, an extremely high value for A_+. The value of A_+ for NaCℓ presents an interesting problem. If Kliewer and Koehler's value of $A_+ \approx 10^4$ is accepted, then A_- must be very small, contrary to the usual belief that they are the same order of magnitude. Kliewer and Koehler reanalyzed their data on the basis of associative interactions between vacancies, thereby obtaining a considerable improvement in the value of

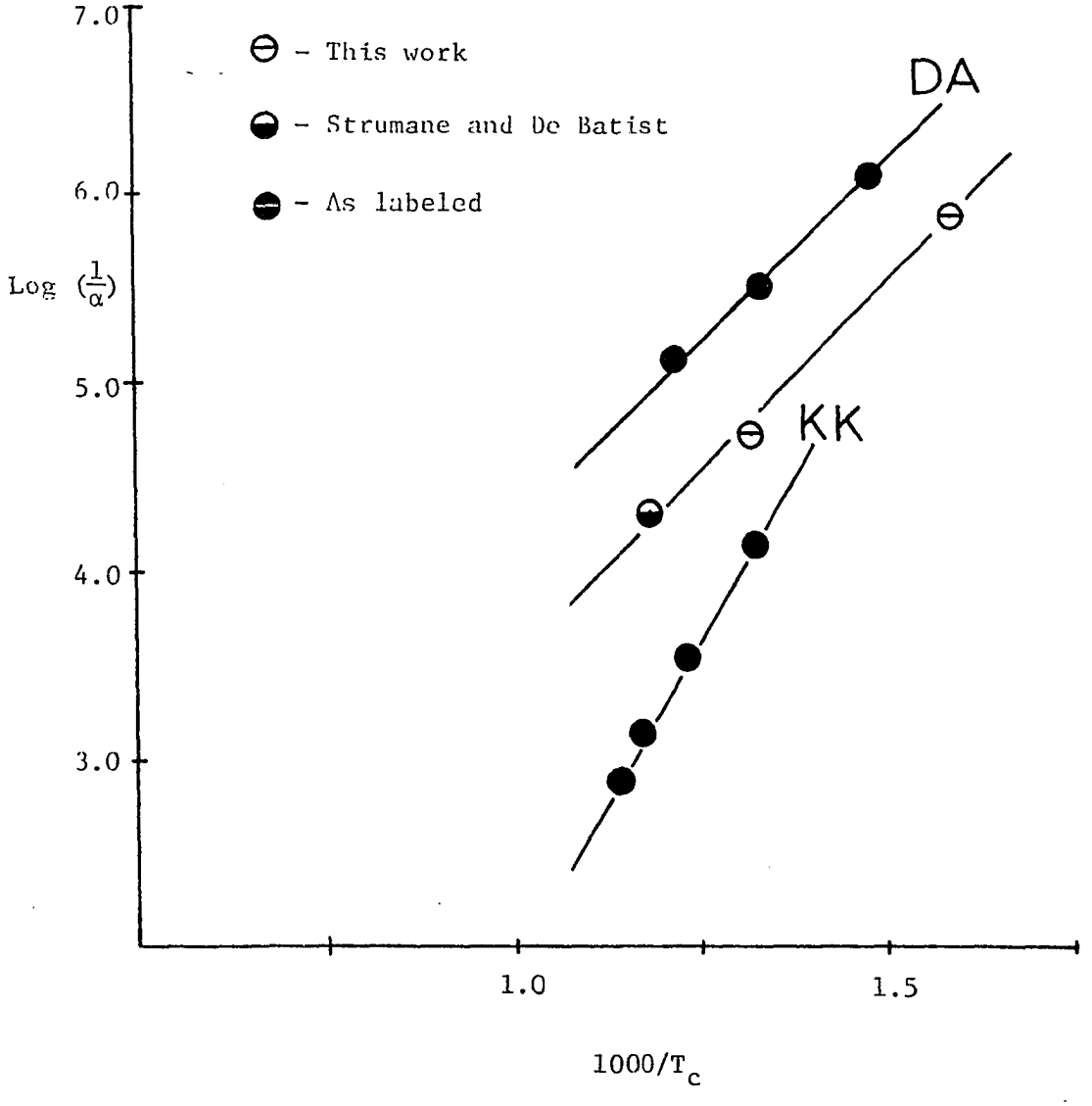

Figure 14. NaCℓ Data

ℓnA_+. Using the improved theory, they found $\ell nA_+ = 6.27$, or $A_+ = 5.2 \times 10^2$. This value still seems unreasonably high, since the accepted value of A_+A_- is 493.[16] Further work, both experimental and theoretical, is needed in this area.

It may be noted that our conductivity data for LiF resulted in a value of E (the Schottky pair formation energy) that was somewhat lower than the value of E = 2.68 eV given by Haven. A recent paper by Boswarva and Lidiard[37] concerning the accurate calculation of E seems to indicate that Haven's value may be too large. Once again it is seen that more recent work on the conductivity parameters of LiF is needed.

It is obvious that many difficulties remain unresolved in the study of interactions of defects in alkali halide crystals. However, charged dislocation studies offer a promising approach to the study of these interactions. The most significant result of the work reported heee then is to indicate the need for continued effort in this field. In particular, for LiF there is a need for repetition of Haven's work and studies of charged dislocations in crystals containing a wide range of divalent metallic impurities. This would be no small task.

Appendix

MATERIAL PREPARATION AND CRYSTAL GROWTH

Introduction

In conjunction with the work reported herein, a series of potassium chloride crystals were grown to aid a similar program. The crystal growth apparatus had been built but never used; a portion of this work was concerned with the modification and perfection of this apparatus, in order to use it to grow the doped potassium chloride (KCℓ) crystals necessary for the above-mentioned work. In addition, the analytical reagent grade KCℓ as received from Mallinkrodt Chemical Company contained impurities which could be removed in this laboratory. Thus, starting with reagent grade KCℓ, it was desirable to chemically purify and distill it in order to obtain clean starting material for growing crystals.

Equipment

The crystal growth apparatus was of the Kyropoulos type, in which the crystal is drawn from the melt. Our technique was to rotate the quartz crucible which contained the melt at 13 revolutions per minute while the crystal puller rod was withdrawn at the rate of 0.125 millimeters per minute. A diagram of the crystal growth apparatus is given in Figure 15.

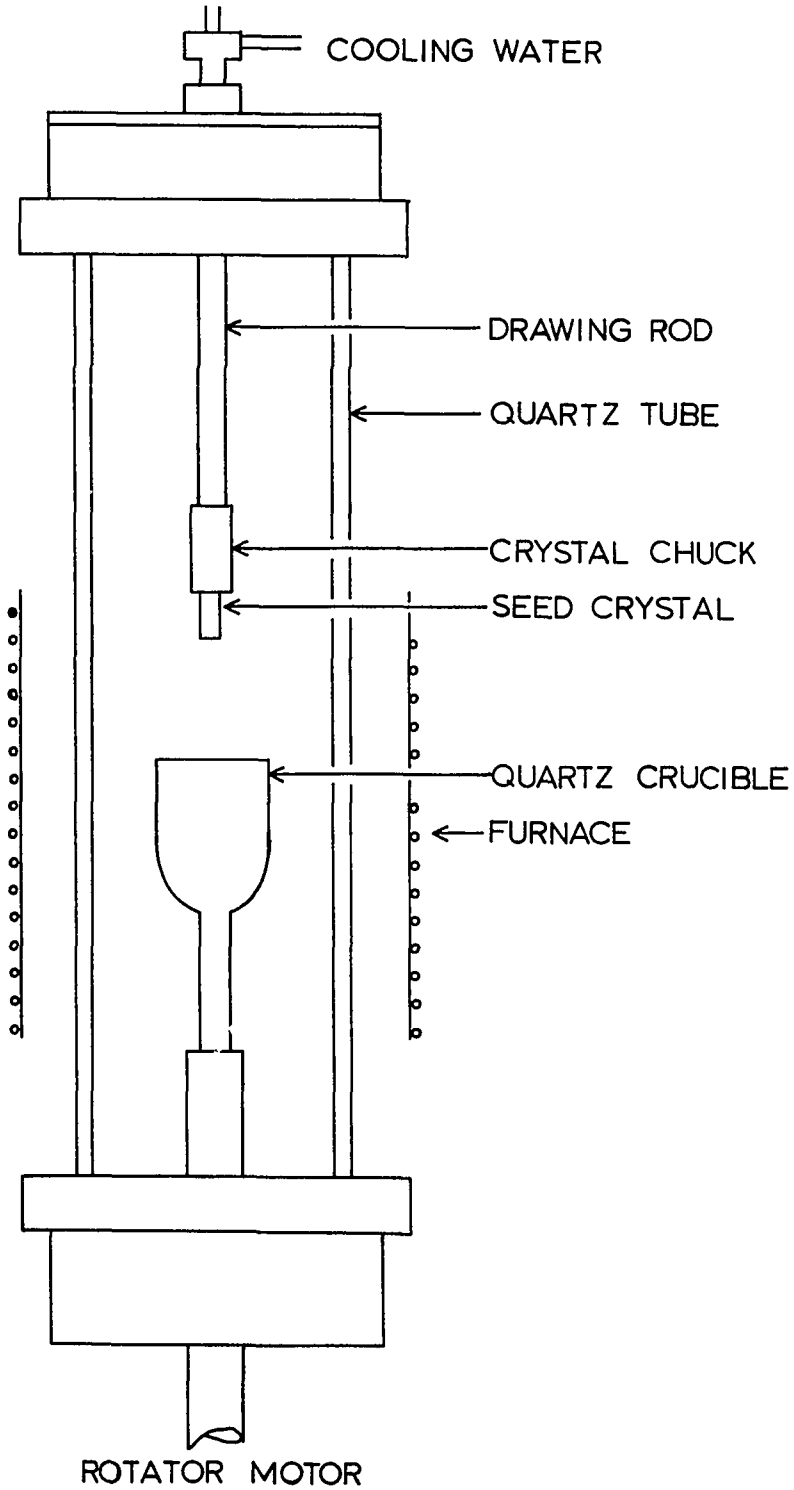

FIGURE 15. CRYSTAL GROWING APPARATUS

The furnace was made of chromel heater wire insulated with ceramic beads and wound on a quartz form; loose asbestos insulated the coils from the outer container of the furnace, which had been formed from stainless steel sheet. Three independent, equal length coils wound adjacent to each other formed the heating elements; separate current adjustments allowed reduction of temperature gradients in the hot zone of the furnace. Since heat loss from the ends is greater than that from the center of the furnace, the end coils were supplied with more power. Set at one inch intervals inside the furnace were 7 chromel-alumel thermocouples, allowing the temperature distribution to be determined over a 6 inch length. The temperature could be held constant to within ±5°C at 800°C over a 4 inch length by carefully adjusting the currents in the coils.

For a temperature control, a resistance thermometer made of platinum wire wound on a ceramic tube formed one leg of a bridge which supplied an error voltage. The platinum thermometer was placed in a quartz tube that was fitted snugly against the furnace windings; the ceramic bead insulation was partially removed to permit intimate contact between the windings and the thermometer.

The error signal fed a transistor amplifier which drove a set of relays capable of controlling 15 amperes in each coil.[38] Rather than interrupt the total current, a one ohm resistance was connected in parallel with the relay contacts, allowing the furnace current to be varied from, say, 11 amperes in the on condition to 10 amperes in

the off condition. This allowed smoother temperature control than complete interruption, but it was necessary to set the furnace current beforehand to correspond approximately to the proper temperature; i.e., 6 amperes through the furnace coils corresponds to a certain temperature, while 7 amperes corresponds to a higher temperature, and the current had to be set so that the temperature reached with the relay contacts open would not exceed the cut-off temperature of the controller.

The quartz tube was closed by end pieces machined from stainless steel; vacuum tight seals were made on the outside by compressing O-rings between the end caps and a threaded aluminum ring. A double O-ring seal packed with Dow-Corning silicone stopcock grease allowed the easy movement of the puller rod in and out of the tube. The puller rod was controlled by a large screw running the length of the assembly; the screw was turned at one revolution every 16:50 minutes when in operation by a small motor-gear combination. A flow of water was maintained in the pull rod to carry off excess heat; in this manner the heat of crystallization was removed from the system. The water was introduced into and removed from the pull rod by flexible plastic tubes.

The lower end piece had an O-ring seal so the crucible support shaft could rotate through it. This seal was well lubricated with Dow-Corning silicone stopcock grease. Both end pieces were built in separate sections so that the actual ends could be removed without disturbing the quartz-stainless steel O-ring seal; they were cooled by a water

flow maintained in copper coils which were silver soldered to the stainless steel sides to prevent the decomposition of O-rings and lubricant. All O-rings were made of Viton-A, and were lubricated with silicone grease.

The crucible was fused onto a long quartz tube, which was held by the slotted stainless steel tube of the crucible support shaft. This arrangement allowed rotation of the crucible, but if binding occurred, the connection would slip rather than break the quartz.

A number of arrangements for holding the seed crystal to the puller rod were tried; initially, a massive piece of pyrolytic carbon was used to clamp the crystal. No external cooling was used in this case; radiation from the carbon was depended upon to carry away the heat of crystallization. This method proved singularly unsuccessful, and water cooling with a smaller carbon chuck was found to be a better design. The final arrangement had a small pyrolytic carbon cylinder threaded tightly onto the puller rod; a hole was drilled along the axis of the cylinder, with two much smaller holes drilled along a diameter. A piece of platinum wire is simultaneously passed through these latter two holes and a small hole drilled in the seed crystal. This proved to be a most successful way to hold the seed in place, but heat dissipation continued to be a problem. A successful approach has been to dip the seed crystal and chuck into the molten salt prior to growth; the salt that freezes onto it makes thermal contact between the two. Excellent crystals have been grown using this technique, but

the practice of dipping carbon into the melt remains dubious, as it could introduce impurities.

Material Preparation (39)

Since the prime object was to remove impurities affecting the electrical characteristics of interest, the use of chelating agents was considered. Chelating agents form stable and highly soluble compounds with polyvalent metal ions in water solution; for example, ethylene diamine tetra acetic acid (EDTA) in a solution of KCℓ made slightly acidic by HCℓ addition will attach the Fe^{+++} ion. If then the KCℓ is precipitated by lowering the temperature, the EDTA + Fe^{+++} combination will remain in solution.

The complete procedure for handling the KCℓ purification is as follows:

1. In one gallon of distilled water one gram of tetrasodium EDTA is dissolved. This will be referred to as the standard solution, and will chelate 2.63×10^{-3} mole of impurity.
2. KCℓ is added to the standard solution at room temperature until saturation is reached.
3. KOH is added at room temperature until a pH of 8 is obtained to remove Ca, Mg, etc.
4. The solution is cooled to its freezing temperature, which precipitates KCℓ. The liquid is decanted.

5. The first four steps are repeated, but modifying step three by adding HCℓ to make the pH equal to 5 rather than repeat the KOH step. This will remove those metals which are removable only in acid solution.

After completion of the EDTA step, the KCℓ was dried at 80°C in a polyethylene container and then stored prior to distillation. The distillation was the final step before growing crystals; it was carried out in the crystal growth apparatus, which was modified for the distillation. For distillation, the system was evacuated; in place of the crystal chuck, a water-cooled stainless steel tube with platinum foil covering its lower 6 inches was used. A charge of purified KCℓ was placed in the quartz crucible and heated to 500°C in a flow of dry nitrogen to remove moisture and excess EDTA. After about five hours at this temperature, the furnace was heated to 900°C, thus starting the distillation. The melt could be observed through an area in the side of the quartz tube enclosing the system. This viewing port was kept clean of KCℓ by directing a bunsen burner flame against it during operation.

The distilled KCℓ was collected on the platinum foil; after completing the distillation, it was removed from the apparatus and stored in plastic bags which were kept in a dessicator.

Crystal Growth

The crystal growth apparatus was first carefully cleaned and dried. Then the purified and distilled KCℓ was placed in the crucible and the temperature of the furnace raised to 100°C for one hour. A pressure of nitrogen of about 5 centimeters of mercury was maintained in the system while raising the temperature. Upon reaching 100°C, the nitrogen was evacuated from the system and replaced. This is recommended as an excellent procedure[40] for the removal of moisture from the crystals. The nitrogen replacement procedure was repeated at 100°C intervals until the melting point of KCℓ was reached. The temperature was then set to about 810°C, and the salt allowed to melt while a constant temperature was established by the temperature control. After the salt was completely melted, the temperature was lowered cautiously toward the melting point; when small crystallites began to form on the surface of the melt (usually after two hours) the temperature was noted and the crystallites remelted by raising the temperature slightly. The seed crystal was then lowered into the melt and closely watched until it could be seen that it was melting; considerable care was needed here, for many seed crystals were lost by not being patient at this point. The temperature was then quickly reduced to slightly above the temperature of crystallite formation. Usually the crystal would begin to form on the seed within 30 minutes; if not, the temperature was lowered until growth occurred. The pulling rod motor was then started; it usually required 4-7 hours to grow a crystal after growth was begun.

After purifying a given batch of material it was desirable to use a seed crystal of this same material with which to grow crystals. This prevented impurities from earlier runs from being introduced into the crystal by impure seeds. Seed crystal growth was accomplished by dipping a platinum rod, which replaced the crystal chuck, into the melt, thereby forming a polycrystalline boule of salt on the rod tip. The extreme end of the boule was then touched to the melt and a thin crystal about 5 millimeters long was grown; it was hoped that in this manner a single crystal would be obtained. The thin section was then widened into a full sized crystal by gradually lowering the temperature while continuing to pull. Single crystals have been grown using this method, although it was more usual to find several orientations. The resulting crystals were used as seeds in growing the crystals of that particular batch.

After the crystal had been grown the puller rod motor and crucible rotation motors were stopped. The temperature controller was connected to a clockdrive motor, which caused the temperature to be lowered by 20°C/hour. This operation prevented strains that might occur in a more violent cooling procedure. After removing the crystal from the grower, it was placed in a dessicator until needed for an experiment.

REFERENCES

1. N. F. Mott and R. W. Gurney, Electronic Processes in Ionic Crystals, 2nd ed. (New York: Dover Publications, Inc., 1964), Chap. 1.

2. Charles Kittel, Introduction to Solid State Physics, 2nd ed. (New York: John Wiley and Sons, Inc., 1956), Chap. 19.

3. A. B. Lidiard, Handuch der Physik, ed. by S. Flugge (Berlin: Springer-Verlag, 1957), XX, p. 258.

4. H. Kelting and R. Witt, Z. Physik 126, 697 (1949).

5. H. G. Van Bueren, Imperfections in Crystals, 2nd ed. (Amsterdam: North-Holland Publishing Co., 1961), p. 142.

6. G. I. Taylor, Proc. Roy. Soc. A145, 362 (1934); E. Orowan, Z. Physik 89, 614 and 635 (1934); M. Polyani, Z. Physik 89, 660 (1934).

7. W. T. Read, Dislocations in Crystals (New York: McGraw-Hill, 1953).

8. A. H. Cottrell, Dislocations and Plastic Flow in Crystals (London: Oxford Press, 1956).

9. J. J. Gilman and W. G. Johnston, Solid State Physics 13, ed. by F. Seitz and D. Turnbull (New York: Academic Press, 1962) p. 148.

10. H. G. Van Vueren, Imperfections in Crystals, 2nd ed. (Amsterdam: North-Holland Publishing Co., 1961), p. 528.

11. A. A. Bruneau and P. L. Pratt, Phil. Mag. 7, 1871 (1962).

12. A. Hikata, C. Elbaum, B. Chick, and R. Truell, J. App. Phys. 34, 2154 (1963).

13. C. Tubandt, Handbuch der Physik, ed. by S. Flugge (Berlin: Springer-Verlag, 1957), XX, p. 258.

14. A. B. Lidiard, Handbuch der Physik, ed. by S. Flugge (Berlin: Springer-Verlag, 1957), XX, p. 258.

15. Y. Haven, Rec. Trav. Chim Pays-Bas. 69, 1471 (1950).

16. R. W. Dreyfus and A. S. Nowick, J. Appl. Phys. supp. 33, 473 (1962).

17. Kurt Lehovic, J. Chem. Phys. 21, 1123 (1953).

18. J. D. Eshelby, C.W.A. Newey, P. L. Pratt, and A. B. Lidiard, Phil. Mag. 3, 75 (1958).

19. H. W. Etzel and R. J. Maurer, J. Chem. Phys. 18, 1003 (1950).

20. Y. Haven, Rec. Trav. Chim. Pays-Bas. 69, 1259 (1950).

21. F. Reuda and W. Dekeyser, Acta, Met. 11, 35 (1963).

22. S. Amelinckx, J. Vennik, G. Remaut, J. Phys. Chem. Solids 11, 170 (1959); G. Remaut, J. Vennik, and S. Amelinckx, J. Phys. Chem. Solids 16, 158 (1960).

23. G. Remaut and J. Vennik, Phil. Mag. 6, 1 (1961).

24. J. E. Caffyn and T. L. Goodfellow, Proc. Phys. Soc. 79, 1285 (1962).

25. R. W. Davidge, Phil. Mag. 8, 1369 (1963).

26. R. W. Davidge, Phys. Stat. Sol. 3, 1851 (1963).

27. R. Strumane and R. DeBatist, Phys. Stat. Sol. 6, 817 (1964).

28. R. J. Schwensfeir, Jr. and C. Elbaum, J. Phys. Chem. Solids 26, 781 (1965).

29. K. L. Kliewer and L. S. Koehler, Phys. Rev. 157, 685 (1967).

30. H. Kanzaki, K. Kido and T. Ninomiya, J. App. Phys. Supp. 33, 482 (1962).

31. R. L. Sproull, Phil. Mag. 5, 815 (1960).

32. Charles E. Skov and Edgar A. Pearlstein, Phys. Rev. 137, A1483 (1965).

33. H. J. Wintle, Can. J. Phys. 45, 2253 (1967).

34. H. S. Ingham, Jr. and R. Smoluchowski, Phys. Rev. 117, 1207 (1960).

35. J. Cotner and J. Weertman, Dislocations in Solids, Discussions of the Faraday Society, Number 38 (London: Butterworth and Co., Ltd., 1964) p. 225.

36. H. Kanzaki, K. Kido, and S. Ohzora, J. Phys. Soc. Japan 18, Suppl. III, 115 (1963).

37. I. M. Boswarva and A. B. Lidiard, Phil. Mag. 16, 805 (1967).

38. E. R. Pike and J. F. Cochran, Rev. Sci. Instr. 31, 1005 (1960).

39. L. W. Watson, private communication.

40. R. W. Dreyfus, The Art and Science of Growing Crystals, ed. by J. J. Gilman (New York: John Wiley and Sons, Inc., 1963) p. 412.